ELSEVIER

Hydrogel machines

Xinyue Liu [1], Ji Liu [1], Shaoting Lin [1], Xuanhe Zhao [1,2,*]

[1] Department of Mechanical Engineering, Massachusetts Institute of Technology, Cambridge, MA 02139, USA
[2] Department of Civil and Environmental Engineering, Massachusetts Institute of Technology, Cambridge, MA 02139, USA

As polymer networks infiltrated with water, hydrogels constitute the major components of the human body; and hydrogels have been widely used in applications that closely interact with biological organisms, such as tissue engineering, drug delivery, and biological research. More recently, owing to their superior softness, wetness, responsiveness, biocompatibility, and bioactivity, hydrogels are being intensively investigated for versatile functions in devices and machines including sensors, actuators, coatings, optics, electronics, and water harvesters. A nascent field named *hydrogel machines* rapidly evolves, exploiting hydrogels as key components for devices and machines. While there are reviews on individual categories of hydrogel machines in literature, a comprehensive discussion on various categories of hydrogel machines that systematically correlate hydrogels' properties and machines' functions is still missing in the field. This review is aimed to provide such a panoramic overview. We first classify various hydrogel machines into a number of categories according to their applications. For each category, we discuss (i) the working principles of the hydrogel machines, (ii) the specific properties of hydrogels that enable the key functions of the machines, and (iii) challenges faced by hydrogel machines and recent developments to address them. The field of hydrogel machines will not only translate fundamental understanding of hydrogels into new applications, but also shift the paradigm in machine design by integrating hydrogels that can potentially minimize physical and physiological mismatches with biological organisms.

Introduction

As hydrophilic polymer networks infiltrated with water, hydrogels behave like both solids and fluids [1,2]. Owing to their cross-linked polymer networks, hydrogels exhibit the properties of elastic solids with deformability and softness [3]. On the other hand, the high water content in hydrogels leads to liquid-like attributes of hydrogels, including permeability to a wide range of chemical and biological molecules [4], and transparency to optical and acoustic waves [5,6]. Beyond these, hydrogels also feature other unique properties, such as swelling and responsiveness [7–9], due to the combination of solid (i.e., polymer networks) and liquid (i.e., water).

Most building blocks of the human body are biological hydrogels (Fig. 1), which are soft, deformable, and contain 60–90 wt% water [2,10–12]). In some sense, the human body is a living machine mainly comprised of hydrogels and skeletons [13]. The nervous system transmits electrical signals and acts as a controller; the digestive and circulatory system transports nutrients, water, and wastes; and the musculoskeletal system functions as motors and actuators. The fact that the human body's functions mainly rely on hydrogels raises an intriguing question in science and technology. While conventional machines are mostly made of rigid elements (e.g., metals, silicon, plastics, and ceramics, Fig. 1), can hydrogels constitute a new class of machines that harness hydrogels' unique properties?

Hydrogels have been widely used in the fields of tissue engineering [10,14–19], cell culture [20–26], and drug delivery

* Corresponding author.
E-mail address: Zhao, X. (zhaox@mit.edu)

 https://doi.org/10.1016/j.mattod.2019.12.026

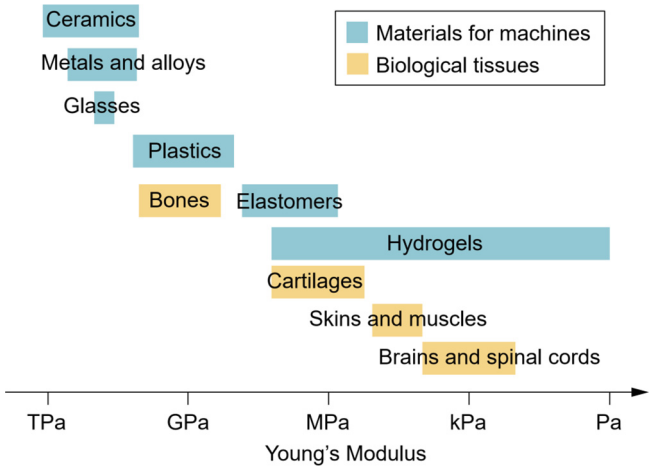

FIGURE 1

Young's moduli of biological tissues and common materials for machines.

[4,27–32], in which the hydrogels intimately interact with biological organisms (Fig. 2). Moreover, the unique properties of hydrogels, such as superior softness, wetness, responsiveness, biocompatibility, and bioactivity [10], indeed suggest the possibility of their crucial functions in devices and machines, such as sensors, actuators, coatings, optics, electronics, and water harvesters [33]. In order to ensure the stable operation of hydrogel machines, it usually requires that the hydrogels are robust in terms of mechanical performance and functionality. Recent innovations in the design of tough hydrogels [34,35], tough adhesion of hydrogels to other engineering materials [36,37], and advanced fabrication methods for hydrogels [38–41] have made hydrogels a promising material candidate for the next-generation machines. A nascent field named *hydrogel machines* rapidly evolves, exploiting hydrogels as key components for devices and machines to potentially replace or complement many conventional machines based on rigid materials.

Whereas individual hydrogel machines such as hydrogel sensors and actuators have been reviewed [33,42,43], a comprehensive overview on various categories of hydrogel machines that systematically correlate hydrogels' properties to machines' functions is still absent in the field. This review is aimed to provide such a panoramic discussion of existing hydrogel machines and a set of rational guidelines for the design of future hydrogel machines based on fundamental thermodynamics, kinetics, chemistries, and mechanics of hydrogels. We first classify various hydrogel machines developed so far into a number of categories according to their major applications, including sensors, actuators, coatings, optics, electronics, and water harvesters (Fig. 2). For each category, we discuss the working principles of hydrogel machines, the unique properties of hydrogels that enable specific functions of the machines, and the challenges faced by hydrogel machines and potential solutions. Lastly, we propose a number of possible directions for the design of next-generation hydrogel machines with high efficiency, robustness, integration, predictability, intelligence, and programmability. Overall, the review will not only summarize a class of new and potentially impactful applications of hydrogels, but also introduce a new paradigm for the design of machines by integrating soft functional materials such as hydrogels.

Hydrogel sensors

By definition, a sensor is a machine or part of a machine that detects and responds to signals in the environments [42]. The human body harbors numerous sensors that can receive environmental signals for perception, such as the eyes for vision, the ears for hearing, the tongue for taste, the nose for smell, and the skin for touch [44]. Conventional sensors, such as electronic sensors and electrochemical sensors, are able to convert environmental inputs to electrical outputs based on semiconductors and/or metallic electrodes. In contrast to conventional sensors made of rigid materials and electrical circuits, hydrogel sensors rely on hydrogels' unique attributes, such as high compliance, high water content, stimuli–responsiveness, and high permeability to a wide range of molecules.

Hydrogel sensors can be classified into two types according to hydrogels' functions in the sensors: (a) stimuli–responsive hydrogels as sensors that can exhibit volume and/or phase changes according to environmental inputs [45–54]; and (b) passive hydrogels as matrices to host responsive substances (e.g., free ions, nanoparticles, biomolecules, and living cells) that respond to environmental inputs [55–57]) (Table 1). The environmental inputs detected by hydrogel sensors include both chemical (e.g., pH, ions, and antibodies) [46,47] and physical (e.g., temperature, light, mechanical stress, and electric field) [49,52,56,58] stimuli. The sensing process of hydrogel sensors usually takes place by first receiving the chemical or physical inputs through chemical diffusion or physical fields, respectively; and then the hydrogel sensors transduce the input signals into measurable outputs [42,59]. The output signals are displayed in the form of geometric, mechanical [46], optical [53], electrical [56], and biological responses of the hydrogel sensors [60]. Hydrogel sensors are becoming practical tools for diverse applications including point-of-care detection, medical diagnostics, and environmental monitoring [61–63].

Stimuli–responsive hydrogels as sensors

The polymer chains and/or polymer networks of stimuli-sensitive hydrogels can be regulated by chemical (e.g., ions, biomolecules) [46,47,64–67] and physical (e.g., temperature, light, mechanical forces, electric fields) [49,50,52,68] stimuli, leading to conformational transformation of polymer chains (e.g., random coil, extended chain, or collapsed globule) and/or changes in the polymer networks (e.g., high or low crosslink density) [42] (Fig. 3a). The molecular level changes of polymer chains and networks result in the micro/macroscopic volume change and/or phase transition of the hydrogels, which can be quantified by instruments such as piezoresistors and transmitted light detectors [59]. Two classical examples of stimuli–responsive hydrogel sensors involve poly(N-isopropylacrylamide) (PNIPAM) hydrogels which have been widely used as temperature sensors (Fig. 3b and c) [69,70], and polyelectrolyte hydrogels which have been adopted to detect variations in pH, ion concentration and electrical potential [45,46,49,58]. In both examples, the polymer chains in the hydrogels experience collapse or extension in

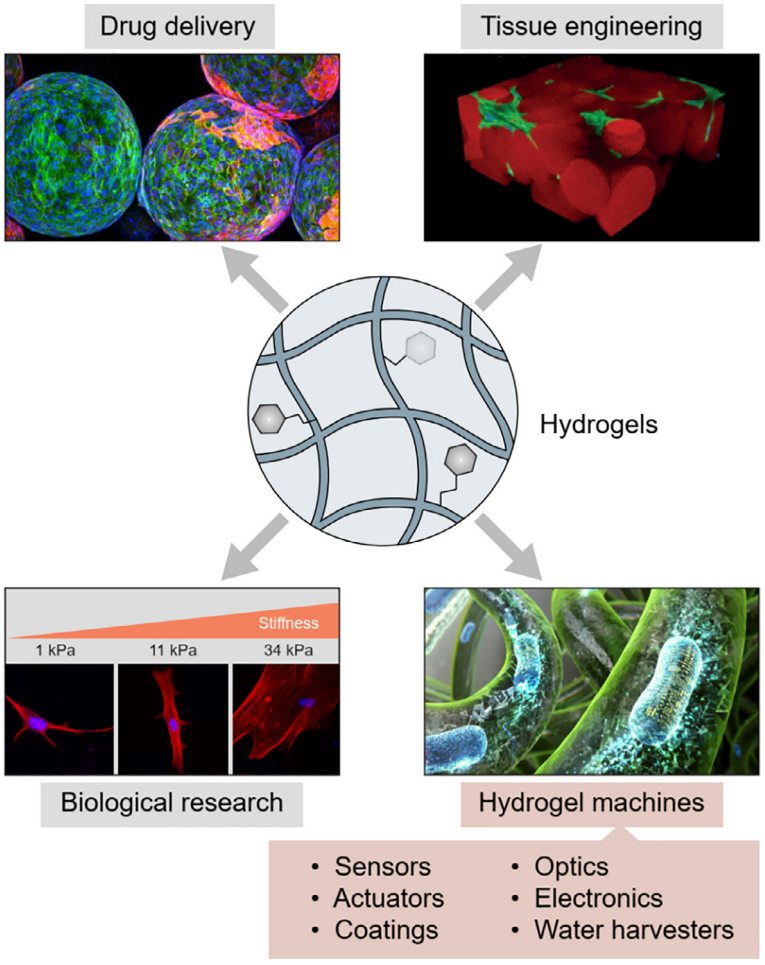

FIGURE 2

Hydrogels have been widely used in the fields such as drug delivery [27,28]), tissue engineering [14], and biological research [20]; and they are being intensively investigated for crucial functions in devices and machines such as sensors, actuators, coatings, optics, electronics, and water harvesters [39]. (Upper left) Adapted with permission from [28]. © 2016 Nature Publishing Group. (Upper right) Adapted with permission from [14]. © 2015 Nature Publishing Group. (Bottom left) Adapted with permission from [20]. © 2006 Elsevier Inc. (Bottom right) Adapted with permission from [39]. © 2017 Wiley-VCH.

response to input signals. As another example, a hydrogel crosslinked by antigens and corresponding antibodies is sensitive to free antigens in the solution, which can bind with antibodies in the network to vary the crosslinking density of the hydrogel and trigger a dramatic change in the hydrogel's volume [47].

Passive hydrogel matrices for sensors

As another strategy for hydrogel sensors, hydrogels can be adopted as inert matrices to accommodate active or responsive elements, such as free ions [56,57]; nanomaterials (i.e., metal and carbon nanomaterials) [71], biomolecules (i.e., enzymes [72–74], antigens/antibodies [75,76], nucleotides [67,77], and fluorescence/luminescence probes [55,78]), and living cells (i.e., bacteria and mammalian cells) [39,60,79]. These active elements are either physically entrapped in or chemically anchored to the hydrogel matrices, and the hydrogel matrices are permeable to chemical inputs (e.g., ions, proteins, carbohydrates, and nucleic acids) [4], thus allowing the interactions between these input signals and the active elements (Fig. 3d). Synthetic hydrogels made of polyethylene glycol (PEG) [80], polyacrylamide (PAAm) [56], or polyvinyl alcohol (PVA) [81,82] are commonly utilized as the passive matrices for active elements. Furthermore, conducting polymer hydrogels are used as matrices to enable rapid electron transfer towards electrodes after the redox reactions between enzymes in hydrogels (e.g., glucose oxidase, lactate oxidase, and uricase) and various biomolecules (e.g., glucose, lactate, and uric acid) [74,83–85]. In contrast to the stimuli–responsive hydrogels, the volume and phase of passive hydrogel matrices usually remain constant during sensing processes. These passive hydrogel matrices can be designed and optimized to achieve desirable properties and structures, such as porosity, biocompatibility, conductivity, and mechanical performance [12,19,86]. For example, Liu et al. reported the encapsulation of genetically engineered bacteria within a tough, stretchable hydrogel-elastomer hybrid [60]. In this living hydrogel sensor, the encapsulated bacteria with programmed genetic circuits are able to express green fluorescent proteins in response to different chemicals (Fig. 3f). The passive hydrogel matrix for the living sensor allows diffusion of water, nutrients, and chemical inputs to the bacteria, and prevents the bacteria leakage toward the environ-

TABLE 1

Representative examples of hydrogel sensors.

Sensor mechanism	Hydrogel	Chemical input	Physical input	Output	Reference
Stimuli–responsive hydrogels as sensors	PAAm-PAA	Ions	/	Geometrical response	[45,46]
	PAAm-protein	Biomolecules	/	Geometrical response	[47,48]
	PAA/PSS/PAMPS	/	Electric field	Geometrical response	[58,98,99]
	PNIPAM	/	Temperature	Geometrical response	[52]
	PNIPAM-PAEMA	/	Temperature	Optical response	[53]
	PAAm-alginate	/	Mechanical forces	Optical response	[50]
	PHEMA-PAA	Ions	/	Optical response	[51]
Passive hydrogel matrices for sensors	PAAm-NaCl/LiCl	/	Mechanical forces	Electrical response	[56,100–102]
	PAAm-AgNW	/	Mechanical forces	Electrical response	[71]
	PAAm-Mo	/	Light	Optical response	[103]
	PAAm-cation receptor	Ions	/	Optical response	[89]
	PEG-glucose fluorescent receptor	Biomolecules	/	Optical response	[55,80,104]
	PAAm-alginate-*E. coli*	Biomolecules	/	Biological response	[60]
	PEG-PPG-*E. coli*	Biomolecules	/	Biological response	[39]
	PEG-cell	Heavy metals	/	Biological response	[79]

PAAm, polyacrylamide; PAA, polyacrylic acid or sodium polyacrylate; PSS, poly(sodium 4-styrenesulfonate); PAMPS, poly(2-acrylamido-2-methyl-1-propanesulfonic acid); PNIPAM, poly(N-isopropylacrylamide); PAEMA, poly(2-aminoethylmethacrylate hydrochloride); PHEMA, poly(hydroxyethyl methacrylate); NaCl, sodium chloride; AgNW, silver nanowire; Mo, ammonium molybdate; *E. coli*, *Escherichia coli*.

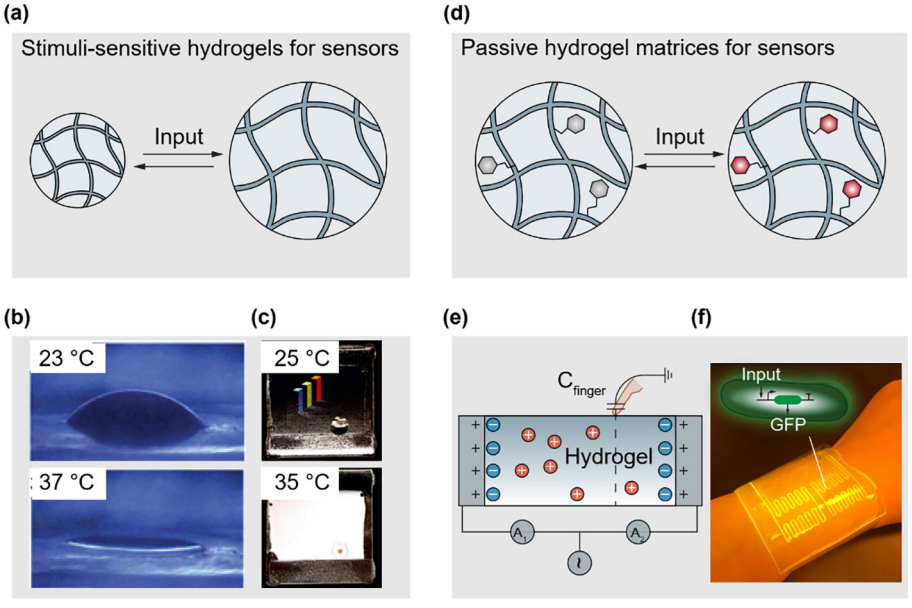

FIGURE 3

Hydrogel sensors based on (a) stimuli–responsive hydrogels as sensors that can exhibit the volume and/or phase change according to the environmental inputs [52–53]), and (d) passive hydrogel matrices for accommodating responsive elements (e.g., free ions, nanoparticles, biomolecules, and living cells) [56,60]. Examples for (a) include (b) temperature-sensitive hydrogels with geometrical response. Adapted with permission from [52]. © 2006 Nature Publishing Group; and (c) temperature-sensitive hydrogels with optical response. Adapted with permission from [53]). © 2019 Elsevier Inc. Examples for (d) include (e) a hydrogel touch panel containing free ions with electrical response. Adapted with permission from [56]. © 2016 American Association for the Advancement of Science; and (f) a living hydrogel sensor containing genetically engineered bacteria with fluorescent response to certain chemicals. Adapted with permission from [60]. © 2017 National Academy of Sciences.

ment [60]. As another example, a work by Kim et al. demonstrated that a highly transparent and stretchable touch panel can be designed with free moving ions in a PAAm hydrogel. The finger position on the touch panel can be interpreted by the current flow in the ionically conductive hydrogels (Fig. 3e) [56].

High-performance sensors commonly exhibit short response time, high sensitivity (i.e., high ratio between output and input signals), low detection limit (i.e., low lower bound of detectable input signals), and high reversibility (i.e., no memory effect caused by previous measurements). Since many hydrogel sensors rely on diffusion of input signals and water in hydrogels, a hurdle for these hydrogel sensors is the long response time, limited by the chemical diffusion across the typical dimensions of hydrogel sensors [87]). To address this challenge, enhancing the chemical's diffusion coefficient in the hydrogel D or decreasing the typical dimension of a hydrogel L can dramatically reduce the diffusion time τ, according to the scaling of diffusion kinetics $\tau \sim L^2/D$ [3]. For a homogeneous, nonporous hydrogel, the mesh size of the hydrogel's polymer network can affect a chemical's diffusion coefficient in the hydrogel, as the mesh size can control steric interactions between the chemical and the polymer network. By reducing polymer and crosslinker concentration in the hydrogel, one can increase the mesh size. The diffusion coefficients of macromolecules in hydrogels can be tuned from 10^{-11} to 10^{-9} m^2 s^{-1} by varying the mesh sizes of the polymer networks [4,88]. On the other side, small-molecule chemicals are usually much smaller than the mesh sizes, so that their diffusion coefficients are almost independent of the mesh sizes, and can be estimated via the Stokes-Einstein equation [4]. Besides the diffusion coefficient; the typical dimension of a hydrogel is another key parameter that controls the response time. For example, a hydrogel antigen sensor with a diameter of 3 mm required more than 1 h to sense biomolecules [47], while hydrogel ion sensors in the form of photonic crystal with a feature size of 500 nm exhibited the color shift in Bragg diffraction within 10 s in response to varied ion concentration [51,89]. To enhance the sensitivity of hydrogel sensors, one strategy is to establish selective and specific interactions (e.g., enzyme–substrate or antigen–antibody interaction) between input signals and stimuli–responsive hydrogels or active elements in passive hydrogels, instead of unspecific interactions. In addition, an abrupt volume change in response to a small change in input signal (e.g., a first-order phase transition such as PNIPAM hydrogels at the lower critical solution temperature) can be introduced to give extreme sensitivity at the critical point [90–92]. For more detailed discussions, please refer to a few reviews on hydrogel sensors [42,59], and specifically on the stimuli–responsive hydrogels [7,93–95] or passive hydrogels that carry nanomaterials [96] and free ions [97].

Hydrogel actuators

An actuator is a machine or a component of a machine that converts other forms of energy into mechanical energy to generate forces and motions. Complex movements of the human body are enabled by the musculoskeletal system as living actuators, in which the skeletal muscles induce forces and motions with short response time (0.1 s) and a large deformation (~40% in strain) [105]). Conventional actuators adapted for mechanical systems usually comprise rigid materials (e.g., metals and ceramics), and their actuation usually relies on relatively small deformations of the rigid materials such as shape memory alloys and piezoelectric ceramics [13,106]. In contrast, actuators made of hydrogels provide mechanical motions commonly driven by relatively large deformations of the hydrogels [107,108]. In the light of different mechanisms for actuation, hydrogel actuators can be divided into three types: (a) stimuli-responsive hydrogels driven by osmotic pressure change [38,52,108–116]; (b) hydrogels matrices incorporating active elements (such as magnetic particles or free ions) in response to varying external fields (such as magnetic or electric fields) [107,117–120]; and (c) hydrogel structures with chambers actuated by hydraulic or pneumatic pressures [5] (Table 2).

Osmotic pressure driven actuators

Osmotic pressure driven hydrogel actuators rely on similar swelling/de-swelling mechanisms as the stimuli–responsive hydrogel sensors discussed above. A wide range of external stimuli, including water [38,121], pH [46,109], biomolecules [47,48,111,122], temperatures [52,70,112,123–126], light [113,127,128], and electric field [49,109,114], can induce the osmotic pressure change of solvents in hydrogels and/or environments, leading to water diffusion in/out of the hydrogels and their corresponding expansion/contraction (Fig. 4a).

Assuming only two species of ions, of valences +1 and −1, are mobile in the hydrogel and in the external solution, the osmotic pressure Π in the hydrogel can be expressed as [129]

$$\Pi = \frac{kT}{v^s}\left[\frac{C^+ + C^-}{C^s} - 2v^s c_0 - \log\frac{v^s C^s}{1+v^s C^s} - \frac{1}{1+v^s C^s} - \frac{\chi}{(1+v^s C^s)^2}\right]$$

where v^s is the volume of a water molecule, C^s, C^+ and C^- are the numbers of water molecules, free cations, and free anions per unit volume of the dry polymer of the hydrogel, c_0 is the number of either specie of ions per unit volume of the external solution, and χ is the interaction parameter between polymer and water. Assuming the fixed charges on the polymer of the hydrogel have valence −1, we further have $C_0 + C^- = C^+$ for charge neutrality inside the hydrogel, where C_0 is the numbers of fixed charges per unit volume of the dry polymer of the hydrogel.

Therefore, osmotic pressure depends on the concentrations of water and various charges, and the interaction parameter between polymer and water. The osmotic pressure of hydrogel can be measured through two methods. A direct method to measure the osmotic pressure involves a semipermeable membrane but is limited by the membrane strength, so that hydrogels of low polymer concentrations or low osmotic pressure can be measured [130,131]. In addition, the osmotic pressure can be indirectly calculated through a few equations of state of hydrogels (e.g., volume conservation and free energy conservation) by subjecting hydrogels to different deformations [132,133].

Tanaka et al. carried out a series of pioneer studies on both thermodynamics and kinetics for volume changes of hydrogels (e.g., PNIPAM, PAAm, and PAA) driven by osmotic pressure [87,90–92]. To further achieve the targeted deformation, such as elongation, bending, folding, twisting, and locomotion, researchers adopted various asymmetric shapes as well as heterogeneous structures for hydrogel actuators through layering, pat-

TABLE 2

Representative examples of hydrogel actuators.

Actuator mechanism	Hydrogel	Input	Actuation force (N)	Actuation frequency (Hz)	Reference
Osmotic pressure driven actuators	PDMAM-NFC	Water	0.001	0.001	[38]
	PAA-PVA	Water	20	0.002	[108]
	PAA-PHEMA	Ions	0.002	0.008	[110]
	PAAm-DNA	Biomolecule	0.002	0.00001	[111]
	PNIPAM	Temperature	0.00001	0.1	[52]
	PNIPAM-TiNS	Temperature	0.001	0.005	[112]
	PAAm-Azo-CD	Light	0.001	0.002	[113]
	PAA-PAAm-Cu	Electric field	0.005	0.01	[109]
	PAMPS	Electric field	0.002	0.1	[114]
Magnetic field driven actuators	Alginate-MNP	Magnetic field	0.1	10	[117]
	PEG-MNP		0.1	0.3	[118]
	PNIPAM-PAAm-MNP		0.00001	2	[119]
Electric field driven actuators (free ions)	PAAm-NaCl	Electric field	0.005	100	[107]
	PAAm-LiCl		0.007	10	[120]
Hydraulic/pneumatic pressure driven actuators	PAAm-alginate	Hydraulic pressure	1	2	[5]

PDMAM, poly(N,N-dimethylacrylamide); NFC, nanofibrillated cellulose; PVA, poly(vinyl alcohol); TiNS, titanate nanosheet; Azo, azobenzene; CD, cyclodextrin; Cu, copper; MNP, magnetic nanoparticle; PEG, polyethylene glycol; LiCl, lithium chloride.

terning, and alignments [38,54,112,123,134]. For instance, Beebe et al. used patterned hydrogel structures as flow control valves in microfluidic channels (Fig. 4b) [110]. Gladman et al. created shape-morphing hydrogel actuators by 3D printing and nanofibril alignment, which can transform into prescribed complex 3D structures upon immersion in water [38]. As another example, Liu et al. developed an ingestible hydrogel device composed of a PVA hydrogel membrane [135] and encapsulated small superabsorbent particles to achieve high swelling ratio, high swelling speed, and long-term robustness. The device can be ingested as a standard-sized pill, swell rapidly into a large soft sphere, and maintain robustness under repeated mechanical loads in the stomach for up to one month (Fig. 4c) [108].

The actuation force and response time are commonly coupled for the osmotic pressure driven hydrogel actuators, where a higher actuation force requires a larger dimension of the hydrogel, leading to longer response time [5]. Therefore, the stimuli–responsive hydrogel actuators are generally hindered by low actuation speed (response time 10 min–10 h) and/or low actuation force (1–10 mN) [112,114,128].

Magnetic or electric field driven actuators

One approach to decouple the actuation forces and times of osmotic pressure driven hydrogel actuators is to embed ingredients that have shorter response time to external inputs in hydrogels, such as magnetic particles in hydrogels in response to magnetic fields [117–119], free ions in ionic conductors in response to electric fields (Fig. 4d and g) [107,120]. The response time of magnetic or electric field driven hydrogel actuators can be as low as 10^{-3} s. In many cases, the short response time may only depend on the mechanical inertia of the hydrogels, instead of their magnetic or electrical properties [107,136,137].

Magnetic hydrogels are hydrogels containing magnetic particles (e.g., magnetite, carbonyl iron, and neodymium-iron-boron) and exhibit unique magnetoelastic properties. Subject to a non-uniform magnetic field, a magnetic hydrogel experiences a body force proportional to the gradient of the applied field, resulting in deformation or motion (Fig. 4d) [117,138]. Zhao et al. showed that the deformation of porous magnetic hydrogels induced by applied magnetic fields could be utilized for controlled drug release (Fig. 4d). The magnetic hydrogel actuators are able to not only complete fast shape transformation (response time 0.1 s) under a constant magnetic field, but also achieve continuous movement according to a rotating magnetic field with the frequency of 2 Hz [117–119]. Ionic conductors composed of free ions in hydrogel matrices (e.g., PAAm) can also exhibit a large deformation actuated by an electric field, when they are assembled with dielectric elastomers [107,120,139]. As illustrated in Fig. 4g, a membrane of a dielectric elastomer is sandwiched between two membranes of hydrogel ionic conductors. When a voltage is applied between the hydrogel ionic conductors, ions of different charge polarities collect on the two surfaces of the dielectric elastomer. The oppositely charged ions attract each other and cause the sandwich to reduce its thickness and increase its area (Fig. 4h) [107].

One challenge for the magnetic and electric field driven actuators is the ability to achieve complex deformation under uniform magnetic and electric fields. To address this, Kim et al. attempted to program ferromagnetic domains in soft materials by 3D printing an elastomeric ink containing ferromagnetic particles, resulting in multiple complex modes of transformation and functions such as jumping, crawling, and rolling (Fig. 2f) [137]. As another example, by assembling an ionically conductive hydrogel film, pre-stretched dielectric elastomers and silicone bodies, Li et al. constructed an untethered soft electronic fish with the ability of fast forward motion underwater, in which the hydrogel and surrounding water served as ionically conductive electrodes (Fig. 2i).

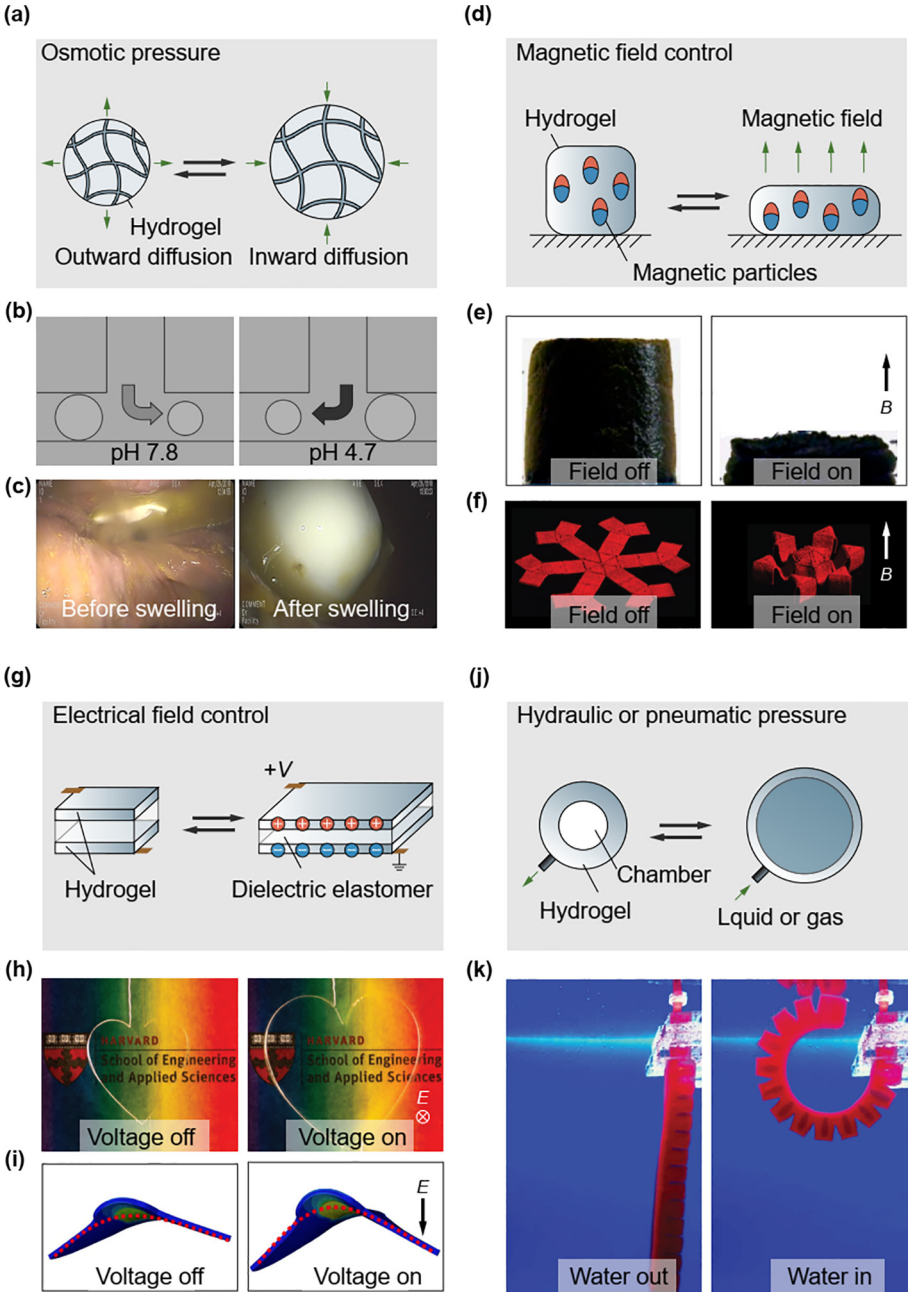

FIGURE 4

Hydrogel actuators based on (a) stimuli–responsive hydrogels driven by osmotic pressure change, (d) hydrogels matrices incorporating magnetic particles controlled by varying magnetic field, (g) hydrogels matrices incorporating free ions controlled by varying electric field, and (j) hydrogel structures with chambers actuated by hydraulic or pneumatic pressures. Examples for (a) include (b) pH-responsive hydrogel actuators as flow control valves in microfluidic channels. Adapted with permission from [110]. © 2000 Nature Publishing Group; and (c) highly swellable hydrogel actuators as ingestible, gastric-retentive devices. Adapted with permission from [108]). © 2019 Nature Publishing Group. Examples for (d) include (e) porous magnetic hydrogel actuators for controlled drug release. Adapted with permission from [117]. © 2011 National Academy of Sciences; and (f) 3D printed ferromagnetic elastomeric actuators capable of fast and complex shape transformation. Adapted with permission from [137]). © 2018 Nature Publishing Group. Examples for (g) include (h) dielectric elastomer-hydrogel actuators capable of fast voltage-induced deformation. Adapted with permission from [107]. © 2013 American Association for the Advancement of Science; and (i) soft electronic fish with the ability of fast forward motion under water. Adapted with permission from [120]. © 2017 American Association for the Advancement of Science. Examples for (j) include (k) hydraulic hydrogel actuators. Adapted with permission from [5]. © 2017 Nature Publishing Group.

Hydraulic or pneumatic pressure driven actuators

Another approach to address the force-speed coupling challenge of osmotic pressure driven hydrogel actuators is to introduce chambers and channels inside hydrogels that can inflate like balloons for actuation (Fig. 4j). Consisting of a bladder (e.g., silicone elastomer) covered in a shell of braided, strong, inextensible fibers (e.g., nylon or metal), the McKibben-type actuators developed by McKibben in the late 1950s is simultaneously strong and fast, similar to muscles [140,141], but their actuation mode is limited to contraction/extension. The elastomer based

pneumatic actuators developed by Whitesides group can give multiple modes of actuation such as contraction, elongation, bending, or rotation by varying the geometry and stiffness of elastomer components [142,143]. Yuk et al. reported the first hydraulic hydrogel actuators, which are made of tough hydrogels with embedded hydraulic chambers and channels. The hydraulic hydrogel actuators showed a much higher actuation force (>1 N) and speed (response time <1 s) than osmotic pressure driven hydrogel actuators (Fig. 4k) [5]. The hydraulic or pneumatic actuation requires mechanical robustness of the assembled hydrogel structures to prevent leakage or failure in the bodies and interfaces [37,144].

Overall, compared to their rigid counterparts, hydrogel actuators have attracted growing interests due to their high flexibility, water contents, and biocompatibility, and resulted in multiple applications, including artificial muscles [113,139], soft robot [5,49], biomedical devices [52,108,117,121], and microfluidics [45,110]. However, the mechanical properties of hydrogels pose significant challenges to the accuracy, reproducibility, and durability of hydrogel actuation. Specifically, unlike the linear elastic materials (e.g., metals and ceramics), the stiffness of hydrogels can vary substantially with increased strain due to the nonlinear elasticity of hydrogels [145], which greatly increases the complexity in modeling and controlling hydrogel actuators. In addition, the design and operation of hydrogel actuators can be further challenged by the viscoelasticity and poroelasticity [145,146], Mullins effect [147], and instability [148] of hydrogels. A better understanding of the fundamental mechanical properties of responsive hydrogels could advance the development of hydrogel actuators with high strain resolution, reproducibility, and robustness, especially for long-term cyclic operations. Please refer to specific reviews for more detailed discussions on hydrogel actuators driven by osmotic pressure [33,54,149,150], magnetic field [151,152], and electric field [97].

Hydrogel coatings

In addition to the responsive components such as sensors and actuators, structural components such as coatings are also crucial to a machine. Many tissues and organs in the human body are covered with hydrogel coatings, resulting in extremely slippery (e.g., friction coefficient 0.002), selectively permeable surfaces [153,154]. For example, mucus on the digestive, respiratory, and reproductive tracts is the primary protection against the external environments [155]. As another example, articular cartilage on bones provides a lubricated surface for smooth joint movement [156]. Similarly, when rigid machines such as orthopedic implants [157,158], neural probes [159,160], cardiac sleeves [161], glucose sensors [162,163], needles [164], catheters [165–167], ultrasound transducers [168], and electrodes for electroencephalogram (EEG), electromyogram (EMG), electrocardiogram (ECG), and transcutaneous electrical nerve stimulation (TENS) [169,170] come into direct contact with the human body, hydrogel coatings can potentially provide a biocompatible interface with minimal mechanical mismatch and foreign body responses [171]. Note that we will specifically focus on hydrogel coatings on machines or engineering components, while hydrogel coatings on biological tissues (e.g., tissue adhesives, tissue sealants, and skin patches) [172,173] will not be covered in this section.

Traditional assembly of different rigid parts in a machine through welding, riveting, or fastening is not applicable to coating hydrogels on machines, owing to the low modulus and high water content of hydrogels. In order to coat hydrogels on engineering materials, including metals [36,164], ceramics [36], glass [36], and elastomers [37], adhesion needs to form between the hydrogels and engineering materials. According to different mechanisms of hydrogel adhesion, we classify hydrogel coatings into four types: (a) physical attached [163,164,168,174], (b) covalent anchored [36,159,161,162,175–177], (c) interfacially interpenetrated [37,144,165,178], and (d) mechanically interlocked [179,180] hydrogel coatings(Table 3).

Physically attached hydrogel coatings

In physically attached hydrogel coatings, only non-covalent interactions, such as electrostatic interactions, van der Waals interactions, hydrogen bonds, and hydrophobic interactions,

TABLE 3

Representative examples of hydrogel coatings.

Coating mechanism	Hydrogel	Thickness (μm)	Interfacial toughness (J/m^2)	Reference
Physically attached coatings	PEG-PPG	20,000	0	[168,174]
	PHEMA	40–120	<10	[164]
	Chitosan-, GelMA, PAA-catechol	200	<10	[163]
Covalently anchored coatings	PEG	20	10–100	[159]
	PCBMA	120	10–100	[162,175]
	PAAm	>100	100	[176]
	PAAm-alginate	>50	>1000	[36,161,177]
Interfacial interpenetrated coatings	Chitosan	>100	10–1000	[178]
	PAAm-alginate	5–25	1000	[165]
	PVA-, PHEMA-cyanoacrylate	>50	500–2000	[144]
Mechanical interlocked coatings	PSS-PDMAEA	>500	10	[179]
	PAAm-PAMPS	>100	200–1000	[180]

PPG, polypropylene glycol; GelMA, gelatin methacrylate; PCBMA, poly(carboxybetaine methacrylate); PDMAEA, poly(2-dimethylaminoethyl acrylate).

exist at the interface between the hydrogel coatings and engineering materials (Fig. 5a). The energies of these interactions are orders of magnitude lower than that of covalent bonds, leading to relatively low interfacial toughness (i.e., lower than 10 J m^{-2}) [36,181] and thus weak adhesion that is easy to detach. The simple attachment and detachment of physically attached hydrogel coatings have enabled several commercial products, such as ultrasound hydrogel pads (e.g., HydroAid) and hydrogel coatings on ECG electrodes (e.g., TenderTrode Plus). These hydrogel coatings can reduce skin irritation and/or increase signal-to-noise ratios, owing to their water contents, compliance, and conformal adhesion on skins (Fig. 5b) [182]. On the other hand, due to the weak adhesion, most of the hydrogel coatings based on non-covalent interactions are limited to short-term applications (e.g., seconds to hours) [164,168].

Covalently anchored hydrogel coatings

Bonding of hydrogels to diverse engineering materials via covalent anchorage can be achieved through different ways of surface functionalization and covalent bonding chemistry (Fig. 5c). Compared to the physical attachment, the covalent anchorage is stronger and more stable under physiological conditions, allowing hydrogel coatings for relatively long-term applications, such as hydrogel coatings on neural implants [159,160]. The robust hydrogel coatings on rigid biomedical devices can provide not only mechanical compliance that matches the tissue modulus and surface lubrication with minimal friction and wear, but also biofunctionalities such as antifouling, minimal immune response, selective permeability, and drug delivery [182,183]. Besides the research advances; covalently anchored hydrogel coatings have been commercialized with products, such as hydrogel coated latex Foley catheter (e.g., Dover) and surgical gloves (e.g., Protexis).

Although covalent anchorage gives more chemically and mechanically stable hydrogel coatings than physically attached ones, the interfacial toughness between the hydrogel layer and the substrate can still be low. As depicted by the Lake-Thomas theory [184], the interfacial adhesion energy is equal to the energy required to fracture a layer of polymer chains, which is in the range of 1–100 J m^{-2}. Such weak and brittle interfaces still induce fracture and/or debonding of hydrogel coatings under high mechanical loads. Yuk et al. first reported a strategy for tough bonding of hydrogels on diverse nonporous solid materials, including metals, ceramics, glasses, and elastomers, by covalently anchoring tough dissipative hydrogels onto the substrates (Fig. 5d) [36]. The energy required for fracturing anchored poly-

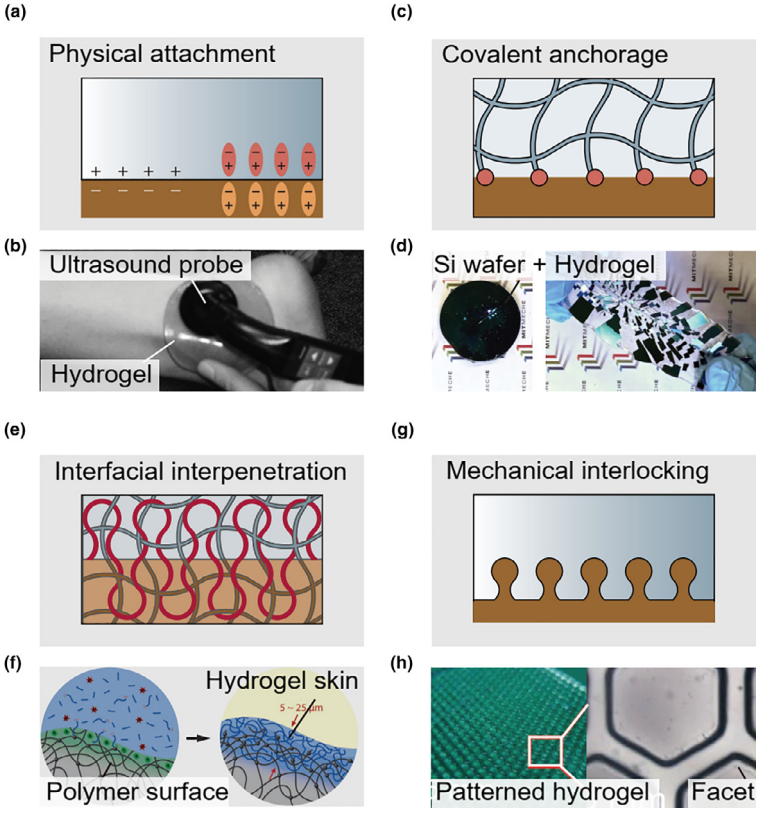

FIGURE 5

Hydrogel coatings based on different mechanisms of hydrogel adhesion, including (a) physical attachment, (c) covalent anchorage, (e) interfacial penetration, and (g) mechanical interlocking. Examples for (a) include (b) hydrogels physically attached on ultrasound probes as ultrasound coupling agents. Adapted with permission from [168]. © 2010 National Athletic Trainers' Association. Examples for (c) include (d) tough hydrogels covalently anchored on the silicon wafers for mechanical protection. Adapted with permission from [36]. © 2016 Nature Publishing Group. Examples for (e) include (f) hydrogel coatings on polymer surfaces of biomedical devices through the interpenetration of hydrogel networks into the polymeric substrates. Adapted with permission from [165]. © 2019 Wiley-VCH. Examples for (g) include (h) hydrogels with microscale facets and grooves for reversible underwater adhesion. Adapted with permission from [179]. © 2018 Wiley-VCH.

mer chains and the energy dissipated in deforming the bulk tough hydrogel synergistically give an interfacial toughness over 1000 J m^{-2}. More recently, Yuk et al. further reported a dry-crosslinking strategy for fast (within 5 s), tough, and long-term stable adhesion of hydrogels on solid materials and tissues [185].

Interfacially interpenetrated hydrogel coatings

Both mechanisms of physical attachment and covalent anchorage for hydrogel coatings described above rely on the introduction of functional groups in hydrogels and/or substrates for adhesion. When the substrate surface is permeable to the polymer chains of hydrogels or bonding agents, interpenetration can form between two polymer networks at the hydrogel-solid interface, resulting in entanglement at the molecular level (Fig. 5e). Yuk et al. proposed that benzophenone treatment of polymers and elastomers can activate their surfaces and make them permeable to hydrophilic polymers and monomers to allow the interpenetration of hydrogel polymer networks into the polymeric and elastomeric substrates (Fig. 5f) [37,165]. As another example, Yang et al. reported that adhesion between two hydrogels can be achieved through the interpenetration of stitching polymers (such as chitosan) into both hydrogels [178].

Mechanically interlocked hydrogel coatings

A rough and porous surface of a machine can enable the mechanical interlocking of hydrogel coatings, which not only increases the interfacial area, but also creates numerous locked snap-fits at the microscale (Fig. 5g). Based on this mechanism, Kurokawa et al. for the first time anchored double network hydrogels to hard, dry, porous substrates, including glass, polyethylene, and sponge [180]. A continuous hydrogel was formed both on top of and in the voids of the porous solid substrates [180]. Inspired from the geometry of Clingfish adhesive disc, Rao et al. fabricated hydrogels with microscale facets and grooves, in which the grooves acted as water drainage channels to facilitate fast contact between the hydrogels and substrates underwater, and the discontinuous facets prevented interfacial crack propagation (Fig. 5h) [179]. Notably, in many cases, mechanical interlocking alone cannot give robust adhesion of hydrogel coatings, since the soft and deformable hydrogels can easily be detached from the snap-fit connectors [181]. Thus, the interlocking mechanism is commonly exploited together with covalent and/or non-covalent interactions for synergistic adhesion [180].

Despite the great advances in hydrogel coatings onto various substrates, there are still some unresolved challenges. One is the ability to conformally and uniformly adapt the hydrogel coatings to devices with complex surface geometries and fine features. Hydrogel coatings fabricated by molding or dip-coating typically result in relatively thick and non-uniform hydrogel layers (over 50 μm), and only applicable for relatively simple surface geometries. A potential solution was reported by Yu et al. by interpenetrating hydrophilic polymers into the surface of diverse polymers with arbitrary shapes to form naturally integrated "hydrogel skins" (Fig. 5f) [165]. Owing to the unique combination of hydrophobic initiators absorbed to the polymer surfaces and hydrophilic initiators dissolved in the hydrogel pre-gel solution, the hydrogel skins with a thickness of 5–25 μm can be formed in situ on the substrates, conformally adapting to complex and fine geometries of diverse polymer materials and devices, such as a polyurethane pacemaker, a silicone Foley catheter, and a swimming robot [165]. More elaborate discussions on different types of hydrogel adhesions and coatings can be found in books and reviews [181,186].

Hydrogel optics

Light and optical techniques have found particular importance in imaging, diagnosis, therapy, surgery, and biological research such as optogenetics and photometry [187]. The eye is a living optical machine, in which the cornea and crystalline lens refract the incoming light rays and focus them on the retina [188]. Cornea and crystalline lens are biological hydrogels containing 78 wt % and 65 wt% water, respectively [189,190]. The high compliance, high water content, and biocompatibility make hydrogels an ideal material candidate for optic devices, especially for those in close contact with biological organisms. Efficient hydrogel optics rely on high transparency (low light absorption and scattering) and high refractive index (low bending loss) of hydrogels [191]. High transparency of hydrogels requires them to be free of light absorbents such as conjugated molecular structures [192], and light scattering domains such as nanoscale inhomogeneity [53]. On the other hand, it usually involves introducing nanostructures or polymers with high molar refractivity to reach a high apparent refractive index of hydrogels [193]. According to their applications, there are four representative types of hydrogel optics developed so far, including (a) ophthalmic lenses [194–198], (b) smart windows and displays [53,56,199], (c) optical fibers [50,79,200], and (d) bioassay matrices [9,201–204] (Table 4).

Ophthalmic lenses

Ophthalmic lenses, including wearable contact lenses [195,196,205]), implantable artificial corneas [198]; intraocular lens [194], and artificial vitreous body [206,207], are traditionally made of rigid transparent materials such as glass, poly(methyl methacrylate), and polycarbonate. Owing to the softness, transparency, oxygen permeability, biocompatibility, and high water content of hydrogels [208,209] (Fig. 6a), the new generation of ophthalmic lenses are mostly based on hydrogels (Fig. 6b–d). For example, the contact lenses made of hydrogels offer an increased level of comfort and hydration for long wearing time (such as 1 day), compared to the traditional poly(methyl methacrylate) ones. In addition, the adaptive hydrogel lenses with adjustable focus lengths have been developed to mimic the lens shape change during eye accommodation [52].

One key challenge in hydrogel lenses is the refractive index of hydrogels. Hydrogels with high water content (60–90 wt%) typically exhibit a refractive index similar to that of water (1.333). However, high refractive indices of lens materials (>1.38) are required in order to make thin lenses, which not only provide the desirable optical correction with a thin film, but also ensure sufficient oxygen permeability and minimal discomfort thanks to low thickness (e.g., ~30 μm) [193]. Therefore, silicone hydrogels, poly(2-hydroxyethyl methacrylate) hydrogels, and their

TABLE 4

Representative examples of hydrogel optics.

Optics type	Hydrogel	Transmittance	Refractive index	Application	Reference
Ophthalmic lenses	PEG-PNVP	< 90%	1.40	Intraocular Lens	[194]
	Silicone-PNVP	~1	1.42	Contact lens	[195–196]
	PHEMA-PNVP	~1	1.38	Contact lens	[195,197]
	PHEMA-PAA-ZnS	~1	1.49	Artificial Cornea	[198]
Smart windows and displays	PNIPAM-PAEMA	85% (25 °C), 0% (35 °C)	1.34 (25 °C), 1.45 (35 °C)	Smart window	[53]
	PAAm-NaCl	~1	1.34	Touch screen	[56,199]
Optical fibers	PEG	~1	1.35	Light guiding	[79,200]
	PAAm-alginate	~1	1.35	Light guiding, sensor	[50]
Bioassay matrices	PAAm-glycerol	~1	1.45	CLARITY	[201,202]
	PAA	~1	1.33	Expansion microscopy	[9]
	PAAm-SDS	~1	1.34	Gel electrophoresis	[203]
	Agarose	<40%	1.33	Gel electrophoresis	[204]

PNVP, poly(N-vinylpyrrolidone); ZnS, zinc sulfide; SDS, sodium dodecyl sulfate.

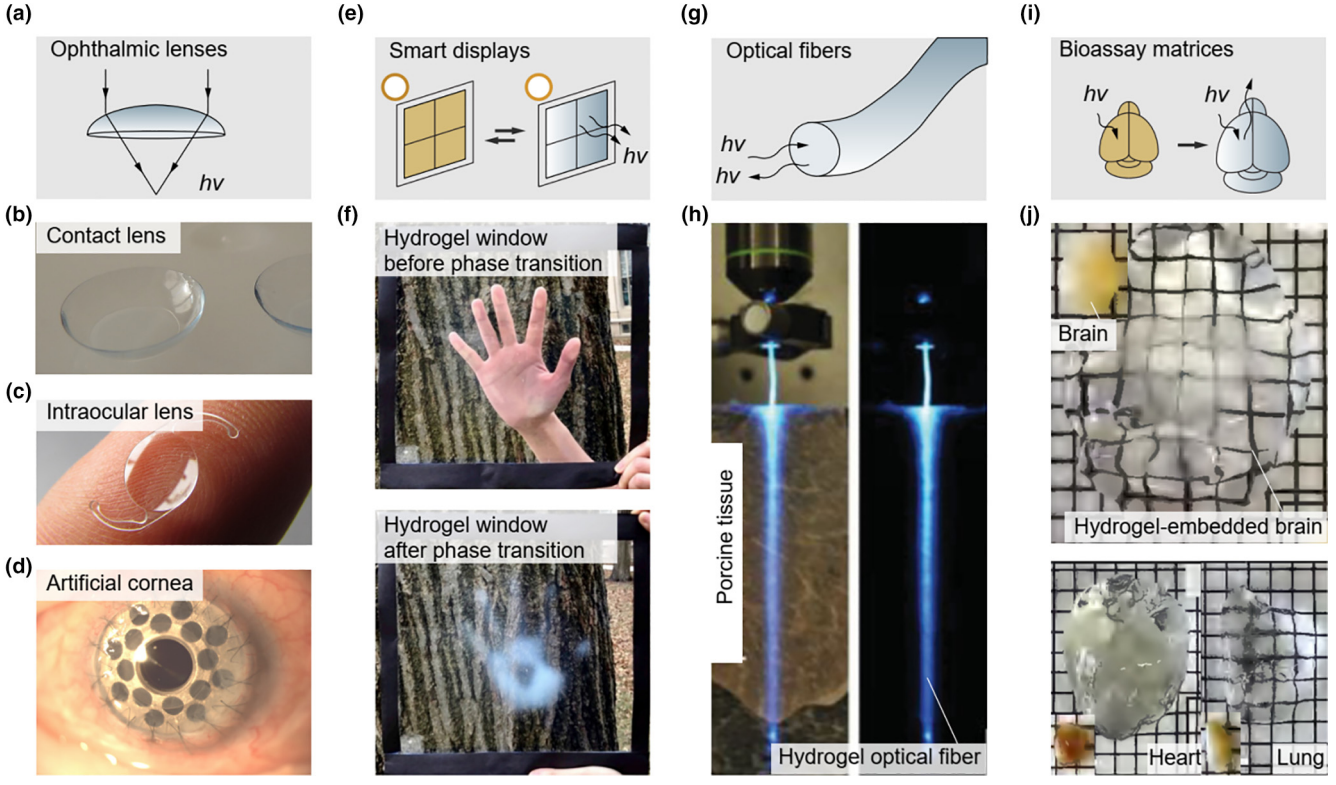

FIGURE 6

Hydrogel optics based on different applications, including (a) ophthalmic lenses, (e) smart windows and displays, (g) optical fibers, and (i) bioassay matrices. *hv*, photon. Examples for (a) include (b) contact lenses, (c) intraocular lenses, and (d) artificial corneas. Adapted with permission from Wikimedia Commons. Examples for (e) include (f) hydrogel smart windows with phase transition induced transparency change. Adapted with permission from [53]. © 2019 Elsevier Inc. Examples for (g) include (h) hydrogel optical fibers for light delivery. Adapted with permission from [200]. © 2015 Wiley-VCH. Examples for (i) include (j) hydrogels as transparent matrices to fix tissues. Adapted with permission from [202]. © 2016 Nature Publishing Group.

derivatives are selected for ophthalmic lenses owing to the reconciled properties of high refractive index (1.380–1.400) and high water content (>60 wt%) [209]. Other strategies that give rise to a high refractive index of hydrogels include the incorporation of inorganic nanoparticles or organic nano-phases featuring high molar refractivity [198,210]. However, the refractive index mismatch between nano-domains/fillers and hydrogel matrices may lead to substantial undesirable light scattering, thus inferior transparency. Downsizing the nano-domains/fillers to less than one-tenth of the wavelength (e.g., zinc sulfide nanoparticles,

3 nm) has been proved to effectively diminish light scattering, and thus achieve a high refractive index of 1.49 and high transparency at the same time [198].

Smart windows and displays

Light management based on smart window technologies is promising, as it can theoretically lead to annual energy savings of more than 1.055×10^{15} kJ in the United States (i.e., 1% of annual total energy consumption) [211]. Materials that can switch light absorption, scattering, and transmission properties in response to external stimuli offer new mechanisms to create smart windows for privacy, comfort, and energy efficiency (Fig. 6e). Traditional transmission modulation mainly relies on inorganic thermochromic or electrochromic materials (e.g., vanadium dioxide, VO_2), which face challenges of high critical temperature (e.g., 68 °C for VO_2) and small transparency change [212,213]. Temperature-responsive hydrogels (e.g., PNIPAM hydrogels) emerge as a promising alternative to inorganic thermochromic materials due to the dramatic phase transition around its lower critical solution temperature (~32 °C, close to the room temperature) [90,112]. For example, Li et al. achieved the tunable scattering of PNIPAM-based hydrogel particles, resulting in thermo-responsive light rejection over the infrared region (Fig. 6f) [53]. That is, the hydrodynamic diameter of these hydrogel particles decreased from 1388 nm at 25 °C to 546 nm at 35 °C, leading to significant infrared light scattering at 35 °C [53]. Furthermore, temperature-regulated solar transmission utilizing PNIPAM hydrogels demonstrated excellent stability, reversibility, and the ability of mass production [53].

In addition, the reversible modulation of light absorption, transmission, or reflection in hydrogels by external signals offers great opportunities in hydrogel based pressure-sensitive touch screen [56,199], and electroluminescent displays [214]. The hydrogel smart windows and displays are soft and stretchable, potentially allowing seamless interfaces for human–machine interactions.

Optical fibers

Optical scattering and absorption of tissues limit the depths of light penetration in tissues, for example, only 50–100 μm for blue light (wavelength of 400–500 nm) and 1–3 mm for red and near infrared light (wavelength of 650–1000 nm) under skin [187]. Optical fibers can be embedded deep in the body to deliver light to or collect optical signals from the body (Fig. 6g). The traditional optical fibers based on glasses and plastics are rigid and static, and thus fail to accompany the natural micro- and/or macro-motions of biological tissues [215]. Owing to the high transparency, low modulus and biocompatibility, hydrogels represent an attractive material candidate for optical fibers in the body, especially for long-term applications. Light-guiding hydrogel fibers enable bidirectional, real-time transmission of optical signals between internal organs and external light sources/detectors [79,200]. Hydrogel optical fibers have recently been implanted in the nervous system for optogenetic modulation and potentially treatment of neuropsychiatric disorders [216,217]. In addition, laser surgeries (e.g., deep tissue ablation, photocoagulation in the retina, and destruction of cardiovascular plaques) and light-activated therapies (e.g., photodynamic therapy) can harness the light delivered through hydrogel fibers [187].

By using PEG hydrogels with high crosslinking density, Choi et al. invented hydrogel optical fibers for in vivo optical sensing and therapy (Fig. 6h) [79,200]. While the PEG hydrogels exhibited high biocompatibility and favorable light-guiding properties [79], they were mechanically brittle and lacked stretchability. Guo et al. used a highly stretchable and tough hydrogel (PAAm-alginate hydrogel) to fabricate optical fibers, attempting to address the low stretchability and brittleness of previous ones [50]. Hydrogel optical fibers with optimized guiding efficiency, mechanical stability, and softness are qualified for light recording and stimulation across an organ-scale distance, and applicable to dynamic and/or fragile tissues such as the brain and spinal cord [79,200].

The applications of hydrogel optical fibers are still facing a number of challenges in terms of long-term optical and mechanical performances. First, when the hydrogel is brought into contact with tissues at its equilibrium state, the refractive index of the fully hydrated hydrogel is usually similar to that of water (1.333), and thus the light can hardly achieve total internal reflection at the interface between hydrogel and the surrounding tissues, leading to severe light leakage. Second, the tissues and hydrogel fibers are in a mechanically dynamic environment, and thus curvatures are generated along the deformed hydrogel fibers, causing aggravated light loss. To address these limitations, various hydrogel fiber structures (e.g., core-cladding geometry [50,200], hydrogel formulations (e.g., nanodomains or nanofillers with high refractive indices [198], fabrication methods (e.g., hydrogels with smooth surfaces [50], and mechanically robust hydrogels (e.g., anti-fatigue hydrogels [135] were developed.

Bioassay matrices

Owing to the optical transparency, molecule permeability, and swelling capability of hydrogels, biologists use them as transparent matrices to fix tissues (Fig. 6i). Two recently invented technologies (i.e., CLARITY [201] and expansion microscopy [9] transform intact tissues with lipids into hydrogel-hybridized forms (i.e., PAAm and PAA hydrogels). Together with antibody or gene based labeling, the resultant hydrogels enable a fine structural analysis of proteins, nucleic acids, and cells in tissues [9,201,202]. Especially, the PAA hydrogels used in the expansion microscopy allow the high-ratio, homogeneous swelling of the tissue specimens when immersed in water for structural observation and analysis with a nanoscale spatial resolution (Fig. 6j) [9]. Besides fixing tissues for imaging, hydrogels are also adopted as a matrix for gel electrophoresis to separate macromolecules (e.g., DNA, RNA, and proteins) based on their sizes and charges under electric fields [203,204]. After electrophoresis, the macromolecules in the transparent hydrogels can be visualized by staining and then viewed under a UV light [203,204].

For more discussions on each type of hydrogel optics, please refer to some specific reviews on contact lenses [208,218], smart windows [219,220], optical fibers [221], and bioassay matrices [222] based on hydrogels.

Hydrogel electronics

The central and peripheral nervous systems in the human body receive, transmit, and generate electrical signals throughout the complex network of neurons in order to collect, process, and respond to information from the environments [223]. While nervous systems in biological organisms are composed of hydrogels (73 wt% water, modulus <3 kPa), existing electronic devices that interact with nervous tissues are mostly based on hard and dry materials such as silicon and metals (0% water, modulus >100 GPa) [182,215]. Due to their similarities to biological tissues and versatility in electrical, mechanical, and biofunctional engineering, hydrogels have recently attracted growing attention in bioelectronics to potentially provide a seamless interface between biology and electronics.

Hydrogels are generally considered as electrical insulators due to the absence of mobile charges or charge carriers. The electrical conductivity of hydrogels in the physiologically relevant conditions is similar to that of tissue media, and much inferior to common electronic conductors such as metals, limiting their applications in electronics [224,225]. To overcome such limitation and enable the possibility of hydrogel electronics for improved tissue-electrode interfaces, a few strategies have been developed to enhance the electrical conductivity of hydrogels, including (a) addition of ionic salts in the hydrogels to achieve ionically conductive hydrogels [56,107,101,102], (b) incorporation of electrically conductive micro- and nano-materials within hydrogel matrices to endow electronic conductivity [71,227–230], and (c) introduction of conducting polymers into hydrogels to enhance electronic conductivity [231–236] (Table 5).

Ionically conductive hydrogels

Ionically conductive hydrogels are enabled by the movement of mobile ionic salts such as Na^+, Li^+, and Cl^- in the hydrogel matrices activated by an electric field (Fig. 7a). The resultant hydrogels can not only maintain the original mechanical compliance and optical transparency, but exhibit high ionic conductivity (~10 S/m when the salt concentration is ~3 M) [101,107]. A series of electronic machines have been developed utilizing the ionically conductive hydrogels, including diodes [237], sensors (Fig. 7b) [56], actuators [107], signal transmitters [136], memristors [238], photovoltaic cells [239], and power sources (Fig. 7c, d) [226]. For example, a power source was created by stacking a high-salinity hydrogel, a cation-selective hydrogel, a low-salinity hydrogel, an anion-selective hydrogel and a second high-salinity hydrogel in sequence (Fig. 7d) [226]. Upon contact with each other, they formed ionically conductive pathways, generating ~150 mV at open-circuit voltage.

One major challenge for applications of ionically conductive hydrogels inside biological organisms is the biocompatibility. The salt concentration in those hydrogels is an order of magnitude higher than the electrolyte concentration in the body fluids (~0.15 M), causing disorders of water and salt metabolism, as well as the loss of conductivity when salts diffuse from hydrogel to extracellular fluid [101,107]. Thereafter, the ionically conductive hydrogels could only be used for non-invasive bioelectronics and machines that do not directly contact with body fluids.

Conductive micro- and nano-composite hydrogels

A variety of carbon and metal micro- and nano-materials, such as silver nanowires [71,240], gold nanoparticles [71], carbon nanotubes [228,241], graphene [229,230], and liquid metals [242] have been incorporated into hydrogels as conductive fillers (Fig. 7e). In those composites, the hydrogel matrices maintain the mechanical properties, while the conductive fillers provide electronic conductivity. Conductive hydrogel-nanomaterial composites have enabled various applications in electronics, including underwater acoustic detectors by depositing silver nanowires on PAAm hydrogel (Fig. 7f) [71], cardiac patches based on gold nanowires in alginate hydrogel or carbon nanotubes in gelatin methacrylate hydrogel [227], skin patches enabled by incorporating wavy titanium wires in PAAm-alginate hydrogel (Fig. 7g) [243], and electrodes for EMG and ECG recording based on graphene nanocomposite hydrogel [244].

However, one obstacle remains in composite hydrogels due to the trade-off between electrical and mechanical properties. To achieve a high electrical conductivity through the micro- or nano-fillers dispersed in the hydrogel matrix, filler concentration

TABLE 5

Representative examples of hydrogel electronics.

Electronics type	Hydrogel	Conductivity (S/m)	Application	Reference
Ionically conductive hydrogels	PAAm-NaCl	10	Actuator, sensor	[100,101,107]
	PAAm-LiCl	10	Signal transmitter, sensor	[102,136]
	PAAm-NaCl, PAMPS, PAPTAC	NA	Power source	[226]
Micro and nanocomposite hydrogels	Alginate-AuNW	NA	Cardiac patch	[227]
	PAAm-AgNW	0.1–10	Microelectrode, acoustic detector	[71]
	Gelatin-CNT	NA	Actuator, microelectrode	[228]
	PAAm-graphene	0.01	Bioelectrode	[229]
	Pure graphene	0.02–0.5	Supercapacitor	[230]
Conducting polymer hydrogels	PNIPAM-PPy	0.8	Responsive electronic device	[233]
	PANI	11	Bioelectrode, supercapacitor	[235,236]
	PAA-PEDOT:PSS	23	Bioelectrode	[234]
	Pure PEDOT:PSS	20–40	Bioelectrode	[231–232]

PAPTAC, poly(3-acrylamidopropyl) trimethylammonium chloride; AuNW, gold nanowire; CNT, carbon nanotube.

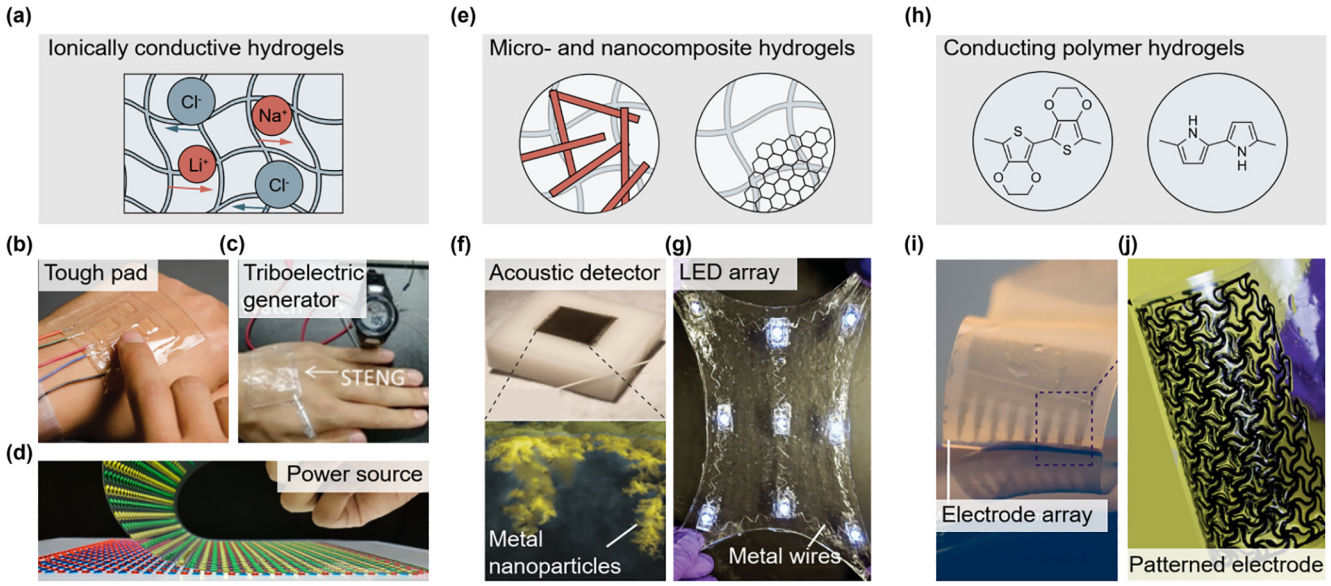

FIGURE 7

Hydrogel electronics based on (a) addition of ionic salts in the hydrogels to achieve ionically conductive hydrogels, (e) incorporation of electrically conductive micro or nanocomposites to endow electronic conductivity, and (h) introduction of conducting polymers into the polymer networks of hydrogel to enhance electronic conductivity. Examples for (a) include (b) touch pads. Adapted with permission from [101]. © 2014 Wiley-VCH; (c) triboelectric generators. Adapted with permission from [102]. © 2017 American Association for the Advancement of Science; and (d) electric-eel-inspired power sources. Adapted with permission from [226]. © 2017 Nature Publishing Group. Examples for (e) include (f) underwater acoustic detectors by depositing silver nanowires on PAAm hydrogel. Adapted with permission from [71]. © 2016 Nature Publishing Group, and (g) skin patches enabled by incorporating wavy titanium wires in PAAm-alginate hydrogel. Adapted with permission from [243]. © 2016 Wiley-VCH. Examples for (h) include (i) PEDOT:PSS hydrogels as elastic microelectronics for low-voltage electrical stimulation. Adapted with permission from [231]. © 2019 Nature Publishing Group, and (j) patterned PEDOT:PSS hydrogel electrode. Adapted with permission from [232]. © 2019 Nature Publishing Group.

above a critical concentration (i.e., percolation threshold) is required [71,230]. On the other hand, a substantially high carbon or metal fraction may give rise to nano/micro-scale aggregates, leading to deteriorated mechanical performances of the hydrogel composite [244].

Conducting polymer hydrogels

The electrical conductivity of conducting polymer hydrogels originates from the high electron mobility within a one-dimensional electronic band formed by the conjugated p-orbitals of conducting polymer chains (Fig. 7h) [245]. Several types of conducting polymers, including poly(3,4-ethylenedioxy thiophene) (PEDOT) [231,232,234], polypyrrole (PPy) [233], and polyaniline (PANI) [235,236], become promising candidates in hydrogel electronics due to their favorable mechanical and electrical properties, electrochemical stability, biocompatibility, and processability for chemical modification [246]. The conducting polymers can either form interpenetrating networks with non-conducting polymer chains/networks [234], or form pure hydrogels without any non-conducting components [231,232]. Poly(3,4-ethylenedioxythiophene):poly(styrene sulfonate) (PEDOT:PSS) hydrogels particularly provide a promising electrical interface with biological tissues for recording and stimulation, in which the coexistence of ionic and electrical conduction ensures a low interfacial impedance [231,232,234]. Existing methods to prepare PEDOT:PSS hydrogels mostly rely on mixing or in situ polymerization of PEDOT:PSS within non-conductive hydrogel templates to form interpenetrating polymer networks (IPN). Feig et al. reported that the interpenetration of a soft and stretchable polymer network within the loosely-crosslinked PEDOT:PSS network led to a conductive IPN hydrogel with low PEDOT:PSS content (1.1 wt%), high conductivity (>10 S m^{-1}), and high stretchability (>100%) [234].

However, many IPN based conducting polymer hydrogels sacrifice their electrical conductivity and/or electrochemical performances since the non-conductive hydrogel network acts as an electrical insulator (e.g., electrical conductivity is typically below 100 S m^{-1} in deionized water) [182,247]. A few strategies have been developed to convert pure PEDOT:PSS solutions into well-dispersed and connected networks, including increasing ionic strength [248], lowering pH [249], and adding ionic liquids [231,250] and co-solvents [251,252]. Recently, Lu et al. showed that the addition of volatile dimethyl sulfoxide in aqueous PEDOT:PSS solutions followed by controlled dry-annealing, and subsequent rehydration can yield pure PEDOT:PSS hydrogels, which exhibited high electrical conductivity (~2000 S m^{-1} in PBS, ~4000 S m^{-1} in deionized water), high stretchability (>35% strain), low Young's modulus (~2 MPa), superior mechanical, electrical and electrochemical stability, and tunable isotropic/anisotropic swelling in wet physiological environments (Fig. 7j) [232]. Moreover, Liu et al. synthesized and used the PEDOT:PSS hydrogels as elastic microelectronics for low-voltage electrical stimulation of the sciatic nerve in mice (Fig. 7i) [231].

More examples and detailed mechanisms of hydrogel electronics and ionotronics can be found in recent reviews by Yuk et al. [182], Yang et al. [97], Koo et al. [253], and Guo et al [254].

Hydrogel water harvesters

Water is critical to the survival of all living organisms. However, only 2.5% of the water on Earth is fresh, and the rest is saline. Furthermore, only 1% of the freshwater is easily accessible, and the majority is trapped in glaciers and groundwater [255]. To enhance accessibility to fresh water, a number of technologies have been developed for water harvesting, including distillation, ion exchange, membrane filtration, and reverse osmosis [256]. Besides these, hydrogels provide alternative methods for water harvesting, owing to the high water content and reversible swelling/dehydration process. Three strategies have been summarized below to harvest freshwater from different sources by hydrogels, including (a) contaminant removal to purify water from polluted water [257–260], (b) desalination by forward osmosis from salt water [261–265], and (c) vapor condensation from atmospheric water [266–269] (Table 6). All three strategies rely on hydrogels' capability of absorbing and releasing water and/or other molecules.

Contaminant adsorption

Each year 1.2 trillion gallons of untreated sewage, stormwater runoff, and industrial waste are dumped into the aquatic system [270]. Heavy metals from mineral processing and dyes from the textile industry are toxic or carcinogenic to aquatic life, and imperil water environment for fishing, swimming, and drinking [271]. A few techniques have been widely adopted to remove the chemical wastes from polluted streams, such as precipitation, adsorption, oxidation, and nanofiltration [272], among which adsorption is viewed as an effective method due to the facile operation, low cost, and adsorbent diversity [272]. Hydrogels have been recognized as a versatile material platform for contaminant adsorption owing to the high water content, rapid ion diffusion, and the ability to incorporate varied functional receptors (Fig. 8a). For example, hydrogels with negatively charged polymer networks (e.g., PAA hydrogel [273], chitosan hydrogel [259,260], and nanocomposite hydrogel258) are able to selectively adsorb water-soluble heavy metal ions (e.g., Cu^{2}+, Pb^{2+}, As^{5+}, and Cr^{6+}) and cationic dyes (e.g., malachite green, methylene blue, basic fuchsin, and crystal violet, Fig. 8b), while hydrogels with positively charged polymer networks (e.g., poly (diallyldimethylammonium chloride)) [274] can adsorb anionic toxins and dyes (e.g., nitrate, phosphate, and methyl orange) via electrostatic interaction. Besides, specific receptors of metal ions and dyes incorporated into the hydrogel networks allow selective recognition and adsorption of these contaminants [258]. The contaminant adsorption from polluted water by hydrogels leads to purified water with a minimal number of contaminants and hydrogels loaded with concentrated contaminants.

The removal efficiency of contaminants depends on the binding affinity between receptors in hydrogels and contaminants in water [258], amounts of receptors, as well as the mesh size of the hydrogels [275]. A high-performance adsorbent requires the hydrogel to exhibit not only high adsorption capacity and rate, but also the regeneration ability for repeated use [258]. A few methods have been reported to regenerate the hydrogel adsorbents after separation of hydrogels from the purified water, such as decreasing pH to release the bounded heavy metal ions from sodium polyacrylate hydrogels [258], and solvent exchange to extract the adsorbed dyes [276]. A few reviews summarized the contaminant and toxin adsorption by hydrogels [277–279].

Desalination

For saline water, the most abundant water source on Earth, hydrogels are used as draw agents for forward osmosis to obtain desalinated water [280]. The hydrogel drawn desalination is accomplished through two steps (Fig. 8c) [262]: First, driven by the osmotic pressure, the hydrogel absorbs clean water from the saline water, in which the hydrogel should possess a higher osmotic pressure than that of saline water. Then, for the purpose

TABLE 6

Representative examples of hydrogel water harvesters.

Water harvester type	Hydrogel	Absorption capacity (g/g)	Absorption time (h)	Release capacity (g/g)	Release time (h)	Reference
Contaminant adsorption	PAAm-laponite	0.05–0.1 (cationic dye)	6	NA	NA	[257]
	PVA-anion receptor	0.0045 (anion)	48	NA	72	[258]
	Gelatin-chitosan	0.070 (heavy metal)	5	NA	NA	[259]
	PAAm-chitosan-EDTA	0.055 (heavy metal)	2	0.051 (heavy metal)	NA	[260]
Desalination	PAA	< 200	NA	NA	NA	[261,262]
	PAA-PNIPAM	15	0.7	9	1 (50 °C)	[263]
	PVA-rGO	3	1	Release rate = 2.5 kg/m^2/h	/	[264]
	PVA-PPy	6	0.5	Release rate = 3.2 kg/m^2/h	/	[265]
Atmospheric water condensation	Alginate-CaCl2	1	10 (26% RH)	0.88	10 (100 °C)	[266]
	PAAm-CNT-CaCl2	1.1	10 (60% RH)	1.06	4.5 (75 °C)	[267]
	PNIPAM-alginate	0.6	0.033 (80% RH)	0.096	0.083 (50 °C)	[268]
	PNIPAM-PPy-Cl	3.4	2 (60% RH)	1.7	0.3 (40 °C)	[269]

EDTA, ethylenediaminetetraacetic acid; rGO, reduced graphene oxide; $CaCl_2$, calcium chloride.

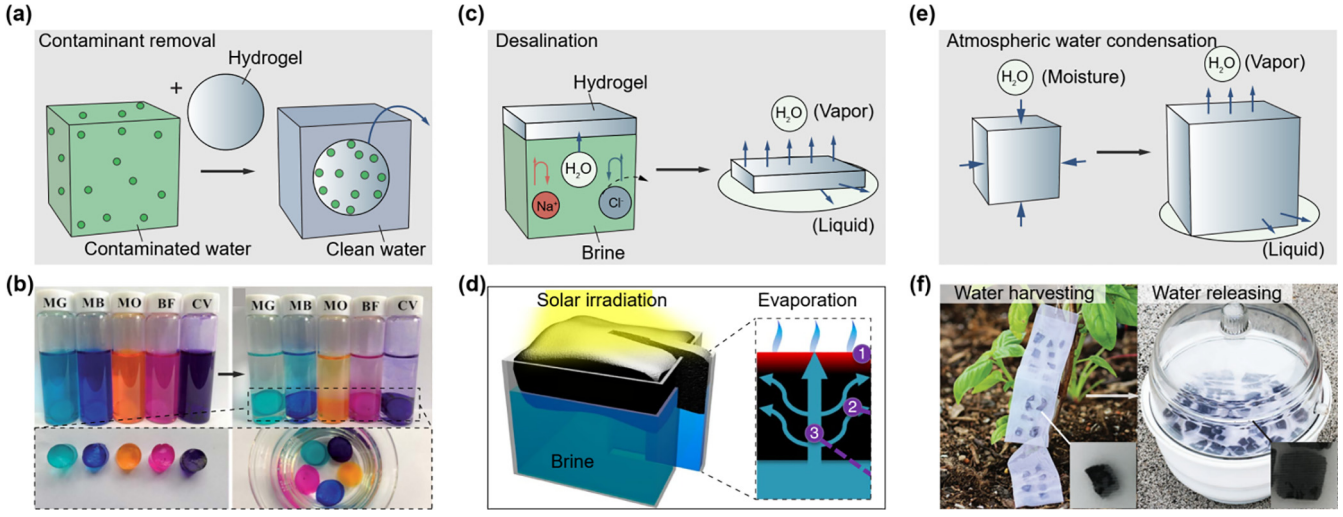

FIGURE 8

Hydrogels water harvesters based on (a) contaminant adsorption, (c) desalination, and (e) atmospheric water condensation. Examples for (a) include (b) hydrogels with negatively charged polymer networks capable of adsorbing various cationic dyes. Adapted with permission from [257]. © 2015 Royal Society of Chemistry. Examples for (c) include (d) nanostructured hydrogels for purifying brine water. Adapted with permission from [265]. © 2018 Nature Publishing Group. Examples for (e) include (f) thermo-responsive hydrogels for atmospheric water harvesting. Adapted with permission from [269]. © 2019 Wiley-VCH.

of pure water recovery and hydrogel re-usage, the captured pure water is subsequently expelled out of the hydrogel by temperature change, applied pressure, or solar irradiation [280]. In a typical work, Li et al. developed a hydrogel composed of PAA-co-PNIPAM, in which the negatively charged polymer chains induce hydrogel swelling with high water flux. Moreover, the swollen hydrogel can release the captured water during the subsequent thermo-induced deswelling [261]. Different hydrogel draw agents, including hydrogel blended with carbon particles for enhanced water recovery [280], hydrogel loaded with magnetic particles for easy retrieval [281], and hydrogels with ionic liquid [282], have been used to increase the desalination efficiency. For more examples, readers can refer to the reviews by Li et al. [283] and Cai et al. [284].

The two separated steps of water absorbing and recovery, however, require repeated swelling/deswelling of the hydrogels, and cannot give continuous desalination process. Zhao et al. demonstrated that a hydrogel with microchannels composed of PVA and polypyrrole allowed continuous purification (Fig. 8d) [265]. In this system, the hydrogel floated in a container of brine, and the capillary microchannels ensured adequate water supply from the bottom to the hydrogel upper surface. Besides, solar irradiation acted as a stimulus for water evaporation from the hydrogel, while polypyrrole as solar absorbers effectively converted solar energy to evaporate water in the hydrogel, leading to a stable, high water vapor collection rate (i.e., 3.2 kg $m^{-2}h^{-1}$ for up to 28 days). The stable evaporation rate revealed that the hydrogel exhibits promising performances for practical long-term solar desalination with antifouling functionality in brine [285–287]. Similar desalination systems based on continuous water supply and solar vapor generation were reported by Yu group using different solar absorbers, including reduced graphene oxide [264], Ti_2O_3 nanoparticles [286], and activated carbon [287].

Atmospheric water condensation

The Earth's atmosphere holds approximately 13 trillion tons of freshwater distributed all over the world with fast replenishment [255]. Atmospheric water harvesting relies on condensing the gaseous water to liquid water, which requires the ability to absorb moisture and then release them in the form of vapor or liquid (Fig. 8e). Deliquescent salts, such as calcium chloride and lithium chloride, exhibit a strong affinity with water and can capture moisture 5–6 times its own weight at low humidity (e.g., 10–25% relative humidity), which is significantly higher than other porous sorbents, such as metal–organic frameworks, molecular sieves, silica gels, zeolite, and activated alumina [288–290]. However, hydration of deliquescent salts after moisture absorption leads to an aqueous solution, which is practically difficult to handle. As an alternative, incorporation of these deliquescent salts within a hydrogel matrix can maintain the hydrated salts in a solid form, without sacrificing the capability of moisture absorption [266,267]. The collected water can be released from the hydrogel at 80–100 °C, assisted by solar irradiation [266,267,291].

The introduction of carbon nanotubes as solar absorbers in the hydrogel enabled almost 100% release of the captured water under regular and even weak sunlight [292]. In order to further lower the energy required for water release, PNIPAM hydrogel was selected as a matrix for the moisture capture due to its drastic change in the hydrophilicity/hydrophobicity by a subtle temperature variation near its lower critical solution temperature. Matsumoto et al. reported that the freeze-dried PNIPAM-alginate hydrogel was able to absorb moisture at 27 °C and 80% RH, while the liquid water oozed out of the hydrogel at 50 °C [268]. Zhao et al. incorporated solar absorbing and hygroscopic polypyrrole chloride into thermo-responsive PNIPAM hydrogels (Fig. 8f) [269]. In these hydrogel systems, liquid water was collected by an oozing process using the thermo-responsive hydrogels with

low energy consumption, because this process got rid of repeated evaporation and condensation for water collection [268,269].

Conclusions and outlook

The last few decades have witnessed explosive development of hydrogel machines in a variety of fields such as soft robotics [139], biomedicine [293], energy [226], and environmental remediation [294]. In particular, the similarity between hydrogels and living tissues in terms of mechanical, chemical, and biological properties makes hydrogels ideal interfaces for the integration of biological and engineering systems [97,182,293]. To enable specific functions of hydrogel machines, hydrogels have been designed to possess specific properties, for instance, stimuli-sensitivity for hydrogel sensors and actuators, strong adhesion for hydrogel coatings, optical transmission for hydrogel optics, electrical conduction for hydrogel electronics, and water absorption/release for hydrogel water harvesters, as summarized in above sections.

Despite great promises and progress of hydrogel machines, there remain a number of unsolved challenges and untapped opportunities, which provide ample room for future research and development, particularly as the field is growing beyond its early stage. Here, we will discuss future research directions for hydrogel machines on five major aspects: (a) new hydrogels with extraordinary properties, (b) hydrogel machines with new functionalities, (c) intelligence and programmability of hydrogel machines, (d) reliability of hydrogel machines, and (e) translation and commercialization of hydrogel machines.

New hydrogels with extraordinary properties

As shown in the discussions above, specific types of hydrogel machines require the hydrogels to possess specific properties. Therefore, the development of new hydrogels with extraordinary properties represents a central need and important future direction of the field.

Slow sensing systems (e.g., >1 h) can no longer match the pace of today's food processing, medical screening, and environmental monitoring. Emerging hydrogel sensors for rapid detection in food, medicine, and environment require stimuli–responsive hydrogels with very short response times (e.g., <10 s) [51]. The actuation power density (i.e., actuation rate × energy density) of mammalian skeletal muscles is over 10^4 W m^{-3}, and this level of power density is highly desirable for artificial muscles used in medical devices, prostheses, and biomimetic robots [105]. However, the power density of existing hydrogel actuators only ranges from 0.1 to 10^3 W m^{-3} [137]. Therefore, the invention of new responsive hydrogels with short response time, high actuation force, and high actuation power density represents a future direction of the field.

Compared with the stiff materials widely adopted in electronic and optic devices, hydrogels still exhibit inferior performances in terms of signal transmission efficiency. For instance, the electrical conductivity of conductive hydrogels (10^{-3}–10^3 S m^{-1}) is orders of magnitude lower than that of the copper (10^7 S m^{-1}) used in printed circuit board [182,245], and the light attenuation in hydrogel optical fibers (10^2 dB m^{-1}) is much higher than that in the silica optical fiber (10^{-4} dB m^{-1}) [295]. Further improvement in machine performance relies on developing new hydrogels with extraordinary physical properties such as electrical and optical properties.

Hydrogel machines with new functionalities

Besides the six categories of hydrogel machines discussed above, there are growing interests and great potentials in developing hydrogel machines with new functionalities. For instance, due to hydrogels' high water contents, the acoustic impedances of hydrogels exhibit nearly perfect match with those of water and soft tissues (1.45–1.70 MPa s m^{-1}) [71]. The impedance match results in the optimal transmission of acoustic waves and negligible acoustic reflection on the interfaces. A number of acoustic devices and machines can be developed based on hydrogels' unique acoustic properties, such as ultrasound coupling agents between probe and skin [296], acoustic camouflages that are undetectable by sonar systems [5,297], and underwater acoustic microphones [71]. As another example, new hydrogel machines may be developed for thermal applications, especially in close contact with human bodies, such as implanted thermometers for long-term temperature monitoring of certain lesions and thermal therapy for cancer treatment. While the thermal conductivity of hydrogels (e.g., 0.6 W m^{-1} K^{-1}) is much lower than those of metals [298–300], engineering the nanofibrous and nanocrystalline structures of hydrogels [135,301] may significantly enhance their thermal conductivities [299,302].

In addition to the hydrogel machines with single functions, the next-generation hydrogel machines are envisioned to carry out a complex series of actions, such as robots and computers. Multiple functions (e.g., sensing, actuation, optical/electrical communication) can be coupled and merged into an integrated system of hydrogel machines, such as electrically conductive hydrogel coatings for epidermal stimulation and recording electrodes [169], and the gastric retentive hydrogel machine that can act as a temperature sensor in the GI tract [108]. More sophisticated hydrogel machines like soft robots for medical operations can perform steering, navigating, sensing, light delivery, electrical stimulation at the same time are expected in the near future [137,303].

Intelligence and programmability of hydrogel machines

Intelligence and programmability are attributes particularly desirable for future hydrogel materials and machines. Progresses towards intelligent and programmable hydrogel machines have been made for years [11,122], and there will be continuous efforts following different strategies, such as bioinspiration, programmed functions, and machine-learning-enabled control and functions.

Living organisms made of soft biological materials give us plenty of inspirations for the design of engineering machines. Existing examples include electrical eels inspired soft batteries [226]; fish inspired swimming robots [120], mussel inspired wet adhesion [304], and pufferfish or tortoise inspired ingestible devices [108,305]. Observing and understanding the functions of nature and biology will provide limitless ideas to design next-generation hydrogel materials and machines.

The programmability of materials refers to the ability to change the materials' properties in a programmable fashion,

based upon user input or autonomous sensing of the materials. There are a few strategies that have been adopted to program the functions of hydrogel machines, including designing responsive hydrogels, fabricating hydrogel microstructures, and genetically engineering building blocks. First of all, hydrogels' unique stimuli–responsiveness provides ample room for the adaptability to various environmental cues (e.g., temperature, moisture, light, pressure, vibration, and electricity) [149]. Second, advanced manufacturing (e.g., 3D and 4D printing) of hydrogels enables precise shape-morphing systems that are useful in smart textiles, autonomous robotics, biomedical devices [38,137]. For these printed hydrogel structures, theory and modeling can help to design prescribed shapes and predict transformations [38,137,356]. Third, genetic engineering of building blocks (such as proteins and nucleic acids) provides new opportunities for developing hydrogels with bottom-up programmed responsiveness and logic operation [39,67,122].

Machine learning has recently found great opportunities in controlling various machines ranging from autonomous cars to smart buildings. Assisted by machine learning, intelligent machines can learn from data, identify patterns, and make decisions with minimal human intervention [306]. Incorporating machine learning to the control system is a promising direction for intelligent hydrogel machines, such as remotely controlled drug vehicles, soft robotics for surgery, and smart windows for building thermal control [307,308]. Machine learning based control approximates a general nonlinear mapping from sensed signals to actuation commands, and the control commands can be continuously updated during the performance evaluation of hydrogel machines [306]. For instance, machine learning algorithms can transform long-term data collected from wearable or implanted hydrogel sensors into scientifically and/or clinically meaningful information, enabling classification of human behaviors, characterization of human habits, and diagnosis of abnormalities and diseases [309,310]. As another example, the intelligent hydrogel actuators can potentially obtain feedbacks from hydrogel sensors in a system, leading to closed-loop operations and/or autonomous behaviors [311].

Reliability of hydrogel machines

With the development of hydrogel machines beyond the early stage, the long-term reliability of hydrogel machines becomes critical in practical applications. For instance, when a hydrogel machine is deployed in the human body, dynamic mechanical loads posed by the skin, muscle, spinal cord, brain, heart, and blood vessels may result in structural degradation of the hydrogel machine over time [215]. Two major considerations, including the mechanical properties of hydrogels and interfacial adhesion between hydrogels and other materials, are of importance to the mechanical reliability of hydrogel machines.

Common hydrogels suffer from the limitation of low mechanical strength and toughness [35,312]. Hydrogels typically composed of a single network are mechanically brittle with fracture energy as low as 0.1–10 J m^{-2} [35]. Following the pioneering work by Gong et al. [34], hydrogels have been made tough to resist crack propagation under a single cycle of mechanical load [35]. The toughening is achieved by incorporating mechanisms for dissipating mechanical energy into stretchable networks of hydrogels [1,357]. However, existing tough hydrogels still suffer from fatigue fracture under multiple cycles of mechanical loads, because the resistance to fatigue crack propagation after prolonged cycles of loads is the energy required to fracture a single layer of polymer chains, which is unaffected by the additional dissipation mechanisms introduced in tough hydrogels [135,313]. Recent studies by Lin et al. showed that the introduction of nanocrystalline domains and aligned nanofibrils in hydrogels can act as the high energy phase to effectively pin fatigue cracks and greatly improve the hydrogels' fatigue resistance [135,301]. The developments and innovations of fatigue-resistant hydrogels will play important roles for the long-term reliability of hydrogel machines under dynamic mechanical loads.

The other aspect of mechanical reliability is associated with hydrogel adhesion, since most hydrogel machines are hybrids of hydrogels and other engineering solids such as metals, elastomers, ceramics, and silicon. These hydrogel-solid hybrids can also be subjected to mechanically dynamic environments, such as cardiac implants on beating hearts and orthopedic implants in moving knees [158,161], where long-term robust adhesion between hydrogels and other solids is critical to the reliability of hydrogels machines. Tough hydrogel adhesion (interfacial toughness >1000 J m^{-2}) has been achieved by the synergistic contribution from the energy dissipation of bulk hydrogels and strong molecular linkage at the hydrogel-solid interfaces [36]. However, such tough hydrogel adhesion still suffers from fatigue failure over multiple cycles of mechanical loads, in which the effect of bulk dissipation has been depleted, leading to the interfacial fatigue threshold on the order of 1–100 J m^{-2}. The design strategy of fatigue-resistant hydrogels by engineering the nanocrystalline domains or nanofibrils in hydrogels [135] can be further extended for the fatigue-resistant hydrogel adhesion by anchoring nanocrystalline domains of hydrogels on solids. These developments in hydrogel adhesion will potentially provide new opportunities for the design of next-generation hydrogel machines [36,37]. In addition, further understanding on mechanical properties of hydrogels (e.g., modulus, maximum strain before rupture, nonlinearity, rate-dependency, hysteresis, resilience, toughness, and fatigue) are crucial not only to ensure long-term reliable hydrogel machines in mechanically dynamic environments, but also to model and predict the deformation and response of hydrogel machines.

Besides the mechanical reliability, the durability of hydrogels in extreme conditions is desirable when hydrogel machines operate in harsh chemical environments (e.g., gastric acid in the stomach) and/or temperatures (e.g., close to freezing point in rivers and seas). Hydrogen bonds have very low association strength in hydrogels due to competition of water for binding sites. Ionic cross-links are vulnerable to mobile ions, which are often encountered under physiological and engineering conditions, leading to degrading performances of hydrogel machines in electrolyte solutions [314]. Low (<0 °C) or high temperature (>100 °C) renders hydrogel machines useless due to the frozen water or evaporated water in hydrogels [315]. Therefore, there is a strong need for hydrogels with good chemical and temperature tolerance.

Translation and commercialization of hydrogel machines

Translation from researches in laboratories to products on the market represents another important future direction for hydrogel machines to make impacts on society. Typical examples of hydrogel products used for biomedical engineering include contact lenses (e.g., Biomedics, Coopervision, SofLens, Bausch and Lomb), ultrasound coupling agents (e.g., Aquaflex, Parker), ultrasound training phantoms (e.g., Zerdine, Cirs), surgical device coatings (e.g., Dover Foley Catheter, Covidien), vascular embolic agents (e.g., LC Beads, BTG; Embosphere, Merit Medical), wound dressings (e.g., Aquaflo, Covidien; Gel 502, First Water), anti-adhesion films (e.g., Seprafilm, Genzyme; Repel-Cv, SyntheMed), dermal fillers (e.g., Restylane, Medicis; Revanesse, Prollenium), breast implants (e.g., Monobloc, Arion), urethral and esophageal bulking agents (e.g., Bulkamid, Contura; Durasphere, Coloplast), artificial cartilages (e.g., Cartiva, Wright Medical), vitreous fillers (e.g., Bio-Alcamid, Polymekon), diapers and feminine hygiene products (e.g., Pampers, Procter and Gamble), and weight control capsules (e.g., Plenity, Gelesis). At the current stage, commercially available hydrogel products are simple and straightforward in terms of chemistry and functionality (Table 7). To ensure the biosafety and biocompatibility, especially for implanted ones, existing hydrogel products are mostly derived from natural polymers, such as alginate, gelatin, hyaluronic acid, cellulose, and collagen. In addition, the existing hydrogel products typically play passive roles as coatings or bulking agents, instead of active, responsive functions.

To pave the way for translation of hydrogel machines developed in academia, understanding practical factors (e.g., cost and availability of raw materials, high-volume manufacturing, size of the market, application scenarios, reliable performance, and safety) will be helpful to turn basic researches into practical

TABLE 7

Examples of recent researches, patents, and commercial products of hydrogel machines.

Hydrogel machine	Mechanism		Research	Patent	Commercial product
Sensors	Stimuli–responsive hydrogels as sensors	Ions	[45,46,51]	[317]	/
		Biomolecules	[47,48]	[318]	Symphony (Echo Therapeutic)
		Temperature	[52,53]	[319]	/
		Light	[113]	/	/
		Mechanical forces	[50]	/	/
		Electric field	[49]	[320]	/
	Passive hydrogel matrices for sensors	Ions	[79,89]	[321]	/
		Biomolecules	[39,55,60,80,104]	[322]	/
		Light	[103]	/	/
		Mechanical forces	[56,71,100–102]	[323]	/
Actuators	Osmotic pressure driven actuators	Water	[38,121]	[324]	/
		Ions	[46,110]	[325,326]	/
		Temperature	[52,70,112,123–126]	[326,327]	/
		Light	[113]	[327]	/
		Electric field	[49,109,114]	[320,328]	/
	Magnetic field driven actuators		[117–119]	[329]	/
	Electric field driven actuators		[107,120]	[323]	/
	Hydraulic/pneumatic pressure driven actuators		[5]	/	/
Coatings	Physical attached coatings		[168,174]	[330]	NeuroPlus (Vermed), Aquaflex (Parker)
	Covalent anchored coatings		[36,37,159,161,162,175–177]	[331,332]	Dover Foley Catheter (Covidien), Surgical Gloves (Cardinal Health)
	Interfacial interpenetrated coatings		[144,165,178]	/	/
	Mechanical interlocked coatings		[179,180]	[333]	/
Optics	Ophthalmic lenses		[198,195,196,334]	[335,336]	Biomedics (Coopervision), SofLens (Bausch and Lomb)
	Smart windows and displays		[53,56,199,213]	[337,338]	/
	Optical fibers		[50,79,200,217]	[6]	/
	Bioassay matrices		[9,201–204]	[339]	Bolt Bis-Tris Plus Gels (ThermoFisher)
Electronics	Ionically conductive hydrogels		[56,107,101,102]	[323]	Ultratrace (Conmed), Tadpole (Neurovision)
	Micro and nanocomposite hydrogels		[71,240,227–231,340–342]	[343]	/
	Conducting polymer hydrogels		[249,231–237,344–347]	[330]	/
Water harvesters	Contaminant removal		[257–261,348–350]	[351]	Waste Lock (M2 Polymer), Kuragel (Kuraray Aqua)
	Desalination		[261–266,352–354]	[355]	/
	Atmospheric water condensation		[266–269]	/	/

products. For hydrogel medical devices, the US Food and Drug Administration evaluates them to assure their safety and effectiveness before commercialization. This evaluation requires a detailed analysis of composition, microbiology, toxicology, immunology, biocompatibility, wear, shelf life, as well as animal tests and clinical investigations. As another example, since hydrogels are susceptible to dehydration in air, most hydrogel machines are limited to be used in a humid environment, such as under water or in human body [5,108]. Advances in anti-dehydration hydrogels through the addition of hygroscopic salts [316] or elastomer covers [37] allow the application of hydrogel machines (e.g., smart windows and displays) when exposed to open air.

Declaration of Competing Interest

The authors declare that they have no known competing financial interests or personal relationships that could have appeared to influence the work reported in this paper.

Acknowledgments

We thank Yoonho Kim and Chi Cheng for insightful and helpful discussions. This work is supported by the National Science Foundation (EFMA-1935291, CMMI-1661627), Office of Naval Research (N00014-17-1-2920), and the U.S. Army Research Office through the Institute for Soldier Nanotechnologies at MIT (W911NF-13-D-0001).

Data Availability

All data generated or analyzed during this study are included in the published article, and are available from the corresponding author on reasonable request.

References

[1] X. Zhao, Soft Matter 10 (5) (2014) 672.
[2] O. Wichterle, D. Lim, Nature 185 (4706) (1960) 117.
[3] W. Hong et al., J. Mech. Phys. Solids 56 (5) (2008) 1779.
[4] J. Li, D.J. Mooney, Nat. Rev. Mater. 1 (12) (2016) 16071.
[5] H. Yuk et al., Nat. Commun. 8 (2017) 14230.
[6] S.-H. Yun, C. Myunghwan, Light-guiding hydrogel devices for cell-based sensing and therapy. Washington, DC: U.S. Patent and Trademark Office (2017)..
[7] R.V. Ulijn et al., Mater. Today 10 (4) (2007) 40.
[8] S.-K. Ahn et al., Soft Matter 4 (6) (2008) 1151.
[9] F. Chen et al., Science 347 (6221) (2015) 543.
[10] K.Y. Lee, D.J. Mooney, Chem. Rev. 101 (7) (2001) 1869.
[11] J. Kopeček, Biomaterials 28 (34) (2007) 5185.
[12] Y.S. Zhang, A. Khademhosseini, Science 356 (6337) (2017) eaaf3627.
[13] B.M. Klebanov et al., Machine Elements: Life and Design, CRC Press, 2007.
[14] D.R. Griffin et al., Nat. Mater. 14 (7) (2015) 737.
[15] J.L. Drury, D.J. Mooney, Biomaterials 24 (24) (2003) 4337.
[16] K.T. Nguyen, J.L. West, Biomaterials 23 (22) (2002) 4307.
[17] A. Khademhosseini, R. Langer, Biomaterials 28 (34) (2007) 5087.
[18] S. Van Vlierberghe et al., Biomacromolecules 12 (5) (2011) 1387.
[19] A.S. Hoffman, Adv. Drug Deliv. Rev. 64 (2012) 18.
[20] A.J. Engler et al., Cell 126 (4) (2006) 677.
[21] S.R. Caliari, J.A. Burdick, Nat. Methods 13 (5) (2016) 405.
[22] N. Huebsch et al., Nat. Mater. 14 (12) (2015) 1269.
[23] O. Chaudhuri et al., Nat. Mater. 15 (3) (2016) 326.
[24] M.W. Tibbitt, K.S. Anseth, Biotechnol. Bioeng. 103 (4) (2009) 655.
[25] M.C. Cushing, K.S. Anseth, Science 316 (5828) (2007) 1133.
[26] V. Jayawarna et al., Adv. Mater. 18 (5) (2006) 611.
[27] A.J. Vegas et al., Nat. Biotechnol. 34 (3) (2016) 345.
[28] A.J. Vegas et al., Nat. Med. 22 (3) (2016) 306.
[29] P. Gupta et al., Drug Discovery Today 7 (10) (2002) 569.
[30] A. Kikuchi, T. Okano, Adv. Drug Deliv. Rev. 54 (1) (2002) 53.
[31] S.W. Kim et al., Pharm. Res. 9 (3) (1992) 283.
[32] Y. Qiu, K. Park, Adv. Drug Deliv. Rev. 53 (3) (2001) 321.
[33] G. Gerlach, K.-F. Arndt, Hydrogel Sensors and Actuators: Engineering and Technology, Springer Science & Business Media, 2009.
[34] J.P. Gong et al., Adv. Mater. 15 (14) (2003) 1155.
[35] J.-Y. Sun et al., Nature 489 (7414) (2012) 133.
[36] H. Yuk et al., Nat. Mater. 15 (2) (2016) 190.
[37] H. Yuk et al., Nat. Commun. 7 (2016) 12028.
[38] A.S. Gladman et al., Nat. Mater. 15 (4) (2016) 413.
[39] X. Liu et al., Adv. Mater. 30 (4) (2018) 1704821.
[40] S. Hong et al., Adv. Mater. 27 (27) (2015) 4035.
[41] B. Grigoryan et al., Science 364 (6439) (2019) 458.
[42] D. Buenger et al., Prog. Polym. Sci. 37 (12) (2012) 1678.
[43] P. Calvert, Adv. Mater. 21 (7) (2009) 743.
[44] M.M. Smith, Sensing the past: seeing, hearing, smelling, tasting, and touching in history, Univ of California Press, 2007.
[45] X. He et al., Nature 487 (7406) (2012) 214.
[46] A. Shastri et al., Nat. Chem. 7 (5) (2015) 447.
[47] T. Miyata et al., Nature 399 (6738) (1999) 766.
[48] J.D. Ehrick et al., Nat. Mater. 4 (4) (2005) 298.
[49] D. Han et al., ACS Appl. Mater. Interfaces 10 (21) (2018) 17512.
[50] J. Guo et al., Adv. Mater. 28 (46) (2016) 10244.
[51] J. Shin et al., Sens. Actuators, B 150 (1) (2010) 183.
[52] L. Dong et al., Nature 442 (7102) (2006) 551.
[53] X.-H. Li et al., Joule 3 (1) (2019) 290.
[54] L. Ionov, Mater. Today 17 (10) (2014) 494.
[55] H. Shibata et al., Proc. Natl. Acad. Sci. U.S.A. 107 (42) (2010) 17894.
[56] C.-C. Kim et al., Science 353 (6300) (2016) 682.
[57] Z. Lei et al., Adv. Mater. 29 (22) (2017) 1700321.
[58] K. Usuki et al., Jpn. J. Appl. Phys. 54 (6S1) (2015) 06FP06.
[59] J. Tavakoli, Y. Tang, Polymers 9 (8) (2017) 364.
[60] X. Liu et al., Proc. Natl. Acad. Sci. U.S.A. 114 (9) (2017) 2200.
[61] S. Perera et al., Antibiotics 7 (3) (2018) 70.
[62] M. Sepantafar et al., Trends Biotechnol. 35 (11) (2017) 1074.
[63] A. Richter et al., Sensors 8 (1) (2008) 561.
[64] G. Zabow et al., Nature 520 (7545) (2015) 73.
[65] E.A. Appel et al., J. Am. Chem. Soc. 134 (28) (2012) 11767.
[66] H.R. Culver et al., Acc. Chem. Res. 50 (2) (2017) 170.
[67] D. Wang et al., Acc. Chem. Res. 50 (4) (2017) 733.
[68] F. Fu et al., Sci. Rob. 3 (16) (2018) eaar8580.
[69] H.G. Schild, Prog. Polym. Sci. 17 (2) (1992) 163.
[70] R. Yoshida et al., Nature 374 (6519) (1995) 240.
[71] Y. Gao et al., Nat. Commun. 7 (2016) 12316.
[72] S.A. Merchant et al., Langmuir 25 (13) (2009) 7736.
[73] C. Eggenstein et al., Biosens. Bioelectron. 14 (1) (1999) 33.
[74] D. Zhai et al., ACS Nano 7 (4) (2013) 3540.
[75] S.D. Carrigan et al., Biomaterials 26 (35) (2005) 7514.
[76] P.T. Charles et al., Biosens. Bioelectron. 20 (4) (2004) 753.
[77] J.S. Kahn et al., Acc. Chem. Res. 50 (4) (2017) 680.
[78] S.M. Borisov et al., Adv. Funct. Mater. 16 (12) (2006) 1536.
[79] M. Choi et al., Nat. Photonics 7 (12) (2013) 987.
[80] Y.J. Heo et al., Proc. Natl. Acad. Sci. U.S.A. 108 (33) (2011) 13399.
[81] T. Fine et al., Biosens. Bioelectron. 21 (12) (2006) 2263.
[82] S. Vaddiraju et al., J. Diab. Sci. Technol. 3 (4) (2009) 863.
[83] Z. Ma et al., Chem. Sci. 10 (25) (2019) 6232.
[84] L. Li et al., Nano Lett. 18 (6) (2018) 3322.
[85] L. Li et al., Nano Lett. 15 (2) (2015) 1146.
[86] N.A. Peppas et al., Annu. Rev. Biomed. Eng. 2 (1) (2000) 9.
[87] T. Tanaka, D.J. Fillmore, J. Chem. Phys. 70 (3) (1979) 1214.
[88] B. Amsden, Macromolecules 31 (23) (1998) 8382.
[89] J.H. Holtz, S.A. Asher, Nature 389 (6653) (1997) 829.
[90] Y. Hirokawa, T. Tanaka, Volume phase transition in a non-ionic gel, in: AIP Conference Proceedings, Aip, 1984, p. 203.
[91] A. Suzuki, T. Tanaka, Nature 346 (6282) (1990) 345.
[92] T. Tanaka et al., Phys. Rev. Lett. 45 (20) (1980) 1636.
[93] G.R. Hendrickson, L.A. Lyon, Soft Matter 5 (1) (2009) 29.
[94] C.D. Jones, J.W. Steed, Chem. Soc. Rev. 45 (23) (2016) 6546.
[95] H.J. van der Linden et al., Analyst 128 (4) (2003) 325.
[96] S. Bhattacharya, S.K. Samanta, Chem. Rev. 116 (19) (2016) 11967.
[97] C. Yang, Z. Suo, Nat. Rev. Mater. 3 (6) (2018) 125.
[98] W. Mohdlsa et al., Sensors 19 (18) (2019) 3967.
[99] R.E. Pelrine et al., Electroactive polymer sensors, Google Patents (2004).

[100] M.S. Sarwar et al., Sci. Adv. 3 (3) (2017) e1602200.
[101] J.Y. Sun et al., Adv. Mater. 26 (45) (2014) 7608.
[102] X. Pu et al., Sci. Adv. 3 (5) (2017) e1700015.
[103] L. Guan et al., React. Funct. Polym. (2019).
[104] A.K. Yetisen et al., Adv. Mater. 29 (15) (2017) 1606380.
[105] T. Mirfakhrai et al., Mater. Today 10 (4) (2007) 30.
[106] J. Huber et al., Proc. R. Soc. London Ser. A: Math. Phys. 453 (1965) (1997) 2185.
[107] C. Keplinger et al., Science 341 (6149) (2013) 984.
[108] X. Liu et al., Nat. Commun. (2019) 10.
[109] E. Palleau et al., Nat. Commun. 4 (2013) 2257.
[110] D.J. Beebe et al., Nature 404 (6778) (2000) 588.
[111] A. Cangialosi et al., Science 357 (6356) (2017) 1126.
[112] Y.S. Kim et al., Nat. Mater. 14 (10) (2015) 1002.
[113] Y. Takashima et al., Nat. Commun. 3 (2012) 1270.
[114] Y. Osada et al., Nature 355 (6357) (1992) 242.
[115] C. Löwenberg et al., Acc. Chem. Res. 50 (4) (2017) 723.
[116] H. Ko, A. Javey, Acc. Chem. Res. 50 (4) (2017) 691.
[117] X. Zhao et al., Proc. Natl. Acad. Sci. U.S.A. 108 (1) (2011) 67.
[118] S.Y. Chin et al., Sci. Rob. 2 (2) (2017) eaah6451.
[119] H.-.W. Huang et al., Sci. Adv. 2 (2) (2017) eaau1532.
[120] T. Li et al., Sci. Adv. 3 (4) (2017) e1602045.
[121] S.Y. Yang et al., Nat. Commun. 4 (2013) 1702.
[122] English, M. A., et al., (2019) 365 (6455), 780..
[123] J. Kim et al., Science 335 (6073) (2012) 1201.
[124] A. Nojoomi et al., Nat. Commun. 9 (1) (2018) 3705.
[125] C. Wang et al., Nature 397 (6718) (1999) 417.
[126] L.-W. Xia et al., Nat. Commun. 4 (2013) 2226.
[127] M. Hippler et al., Nat. Commun. 10 (1) (2019) 232.
[128] E. Wang et al., Nano Lett. 13 (6) (2013) 2826.
[129] W. Hong et al., J. Mech. Phys. Solids 58 (4) (2010) 558.
[130] P.J. Flory, J. Chem. Phys. 13 (11) (1945) 453.
[131] J.C. Day, I.D. Robb, Polym. Gels Networks 22 (11) (1981) 1530.
[132] S. Cai, Z. Suo, Europhys. Lett. 97 (3) (2012) 34009.
[133] J. Li et al., Soft Matter 8 (31) (2012) 8121.
[134] S.-J. Jeon et al., Acc. Chem. Res. 50 (2) (2017) 161.
[135] S. Lin et al., Sci. Adv. 5 (1) (2019) eaau8528.
[136] C.H. Yang et al., Extreme Mech. Lett. 3 (2015) 59.
[137] Y. Kim et al., Nature 558 (7709) (2018) 274.
[138] M. Zrínyi et al., J. Chem. Phys. 104 (21) (1996) 8750.
[139] N. Kellaris et al., Sci. Rob. 3 (14) (2018) eaar3276.
[140] B. Tondu, P. Lopez, IEEE Control Syst. Mag. 20 (2) (2000) 15.
[141] H.A. Baldwin, Realizable models of muscle function, in: Biomechanics, Springer, 1969, p. 139.
[142] F. Ilievski et al., Angew. Chem. Int. Ed. 50 (8) (2011) 1890.
[143] B. Mosadegh et al., Adv. Funct. Mater. 24 (15) (2014) 2163.
[144] D. Wirthl et al., Sci. Adv. 3 (6) (2017) e1700053.
[145] Y. Mao et al., J. Mech. Phys. Solids 100 (2017) 103.
[146] Y. Hu et al., Appl. Phys. Lett. 96 (12) (2010) 121904.
[147] T. Zhang et al., Extreme Mech. Lett. 4 (2015) 1.
[148] S. Lin et al., J. Mech. Phys. Solids 106 (2017) 229.
[149] O. Erol et al., Adv. Mater. Technol. 4 (4) (2019) 1900043.
[150] L. Ionov, Adv. Funct. Mater. 23 (36) (2013) 4555.
[151] M. Zrinyi et al., Polym. Gels Networks 5 (5) (1997) 415.
[152] P. Ilg, Soft Matter 9 (13) (2013) 3465.
[153] D. Accoto et al., Measurements of the frictional properties of the gastrointestinal tract, World Tribology Congress, 2001.
[154] F. Guilak, Arthritis Rheum. 52 (6) (2005) 1632.
[155] O. Lieleg, K. Ribbeck, Trends Cell Biol. 21 (9) (2011) 543.
[156] A.J. Sophia Fox et al., Sports Health 1 (6) (2009) 461.
[157] L. Drago et al., Clin. Orthop. Related Res. 472 (11) (2014) 3311.
[158] S.B. Goodman et al., Biomaterials 34 (13) (2013) 3174.
[159] K.C. Spencer et al., Sci. Rep. 7 (1) (2017) 1952.
[160] R. Green, M.R. Abidian, Adv. Mater. 27 (46) (2015) 7620.
[161] E.T. Roche et al., Sci. Transl. Med. 9 (373) (2017) eaaf3925.
[162] W. Yang et al., Biosens. Bioelectron. 26 (5) (2011) 2454.
[163] B. Yu et al., Biosens. Bioelectron. 23 (8) (2008) 1278.
[164] M. Shin et al., Nat. Mater. 16 (1) (2017) 147.
[165] Y. Yu et al., Adv. Mater. 31 (7) (2019) 1807101.
[166] J.E. Shapland et al., Phoretic Balloon Catheter with Hydrogel Coating, U.S. Patent and Trademark Office, Washington, DC, 1997.
[167] R. Sahatjian, Drug Delivery System Making Use of a Hydrogel Polymer Coating, U.S. Patent and Trademark Office, Washington, DC, 1994.
[168] D.O. Draper et al., J. Athl. Train. 45 (4) (2010) 333.
[169] K. Nagamine et al., Sens. Actuators, B 237 (2016) 49.
[170] T. Shay et al., Soft Matter 14 (17) (2018) 3296.
[171] L. Zhang et al., Nat. Biotechnol. 31 (6) (2013) 553.
[172] J. Li et al., Science 357 (6349) (2017) 378.
[173] N. Annabi et al., Sci. Transl. Med. 9 (410) (2017) eaai7466.
[174] H. Cheng et al., ACS Appl. Mater. Interfaces 9 (13) (2017) 11428.
[175] W. Yang et al., Biomaterials 33 (32) (2012) 7945.
[176] Q. Liu et al., Nat. Commun. 9 (1) (2018) 846.
[177] G.A. Parada et al., Adv. Healthcare Mater. 6 (19) (2017) 1700520.
[178] J. Yang et al., Adv. Mater. 30 (25) (2018) 1800671.
[179] P. Rao et al., Adv. Mater. 30 (32) (2018) 1801884.
[180] T. Kurokawa et al., Acta Biomater. 6 (4) (2010) 1353.
[181] J. Yang et al., Adv. Funct. Mater. (2019) 1901693.
[182] H. Yuk et al., Chem. Soc. Rev. (2019).
[183] P. Krsko, M. Libera, Mater. Today 8 (12) (2005) 36.
[184] G. Lake, A. Thomas, Proc. R. Soc. Lond. A 300 (1460) (1967) 108.
[185] H. Yuk et al., Nature 575 (7781) (2019) 169.
[186] R.J. LaPorte, Hydrophilic polymer coatings for medical devices, Routledge, 2017.
[187] S.H. Yun, S.J. Kwok, Nat. Biomed. Eng. 1 (1) (2017) 0008.
[188] J.F. Koretz, G.H. Handelman, Sci. Am. 259 (1) (1988) 92.
[189] H. Davson, Biochem. J 59 (1) (1955) 24.
[190] R. Fisher, B.E. Pettet, J. Physiol. 234 (2) (1973) 443.
[191] Keiser, G., Wiley Encyclopedia of Telecommunications (2003)..
[192] E.R. Blout et al., J. Am. Chem. Soc. 70 (1) (1948) 194.
[193] C. Lü, B. Yang, J. Mater. Chem. 19 (19) (2009) 2884.
[194] J.H. de Groot et al., Biomacromolecules 2 (3) (2001) 628.
[195] J.J. Nichols, D.A. Berntsen, Ophthal. Physiol. Opt. 23 (6) (2003) 517.
[196] M. Lira et al., Contact Lens Anterior Eye 31 (2) (2008) 89.
[197] F. Kaynak Onurdağ et al., Graefe's Arch. Clin. Exp. Ophthalmol. 249 (4) (2011) 559.
[198] Q. Zhang et al., ACS Macro Lett. 1 (7) (2012) 876.
[199] Y. Lee et al., Nat. Commun. 9 (1) (2018) 1804.
[200] M. Choi et al., Adv. Mater. 27 (27) (2015) 4081.
[201] K. Chung et al., Nature 497 (2013) 332.
[202] T. Ku et al., Nat. Biotechnol. 34 (2016) 973.
[203] H. Schägger, G. von Jagow, Anal. Biochem. 166 (2) (1987) 368.
[204] C.-B. Laurell, Anal. Biochem. 15 (1) (1966) 45.
[205] C. Karlgard et al., Int. J. Pharm. 257 (1–2) (2003) 141.
[206] Z. Liu et al., *Nat. Biomed. Eng.* (2019).
[207] K. Hayashi et al., Nat. Biomed. Eng. 1 (3) (2017) 0044.
[208] P.C. Nicolson, J. Vogt, Biomaterials 22 (24) (2001) 3273.
[209] D. Myung et al., Biotechnol. Prog. 24 (3) (2008) 735.
[210] H.M. Reinhardt et al., J. Mater. Sci. 51 (22) (2016) 9971.
[211] Apte, J., and Arasteh, D., (2008)..
[212] Y. Gao et al., Nano Energy 1 (2) (2012) 221.
[213] T.-G. La et al., ACS Appl. Mater. Interfaces 9 (38) (2017) 33100.
[214] C.H. Yang et al., Adv. Mater. 28 (22) (2016) 4480.
[215] S.P. Lacour et al., Nat. Rev. Mater. 1 (10) (2016) 16063.
[216] H. Sheng et al., Extreme Mech. Lett. 30 (2019) 100510.
[217] L. Wang et al., Adv. Opt. Mater. 6 (16) (2018) 1800427.
[218] E. Caló, V.V. Khutoryanskiy, Eur. Polym. J. 65 (2015) 252.
[219] H.N. Kim, S. Yang, Adv. Funct. Mater. (2019) 1902597.
[220] Y. Ke et al., Adv. Energy Mater. (2019) 1902066.
[221] M.G. Kuzyk, Polymer Fiber Optics: materials, physics, and applications, CRC Press, 2018.
[222] D.S. Richardson, J.W. Lichtman, Cell 162 (2) (2015) 246.
[223] J.B. Ranck Jr, Brain Res. 98 (3) (1975) 417.
[224] J. Gong et al., J. Phys. Chem. B 101 (5) (1997) 740.
[225] H. Li et al., Macromolecules 49 (23) (2016) 9239.
[226] T.B.H. Schroeder et al., Nature 552 (2017) 214.
[227] T. Dvir et al., Nat. Nanotechnol. 6 (2011) 720.
[228] S.R. Shin et al., ACS Nano 7 (3) (2013) 2369.
[229] H. Jo et al., Acta Biomater. 48 (2017) 100.
[230] Y. Xu et al., ACS Nano 4 (7) (2010) 4324.
[231] Y. Liu et al., Nat. Biomed. Eng. 3 (1) (2019) 58.
[232] B. Lu et al., Nat. Commun. 10 (1) (2019) 1043.
[233] Y. Shi et al., Adv. Funct. Mater. 25 (8) (2015) 1219.
[234] V.R. Feig et al., Nat. Commun. 9 (1) (2018) 2740.
[235] L. Pan et al., Proc. Natl. Acad. Sci. U.S.A. 109 (24) (2012) 9287.
[236] J. Stejskal et al., Macromolecules 31 (7) (1998) 2218.
[237] O.J. Cayre et al., J. Am. Chem. Soc. 129 (35) (2007) 10801.
[238] H.J. Koo et al., Adv. Mater. 23 (31) (2011) 3559.

[239] H.-J. Koo et al., J. Mater. Chem. 21 (1) (2011) 72.
[240] X. Jing et al., Mater. Lett. 237 (2019) 53.
[241] L. Mottet et al., Soft Matter 14 (8) (2018) 1434.
[242] H. Peng et al., Mater. Horiz. 6 (3) (2019) 618.
[243] S. Lin et al., Adv. Mater. 28 (22) (2016) 4497.
[244] L. Han et al., Small 13 (2) (2017) 1601916.
[245] R. Gangopadhyay, A. De, Chem. Mater. 12 (3) (2000) 608.
[246] F. Zhao et al., Acc. Chem. Res. 50 (7) (2017) 1734.
[247] A.K. Gaharwar et al., Biotechnol. Bioeng. 111 (3) (2014) 441.
[248] M.A. Leaf, M. Muthukumar, Macromolecules 49 (11) (2016) 4286.
[249] B. Yao et al., Adv. Mater. 29 (28) (2017) 1700974.
[250] Y. Wang et al., Sci. Adv. 3 (3) (2017) e1602076.
[251] Q. Wei et al., Adv. Mater. 25 (20) (2013) 2831.
[252] J.P. Thomas et al., J. Mater. Chem. A 2 (7) (2014) 2383.
[253] H.-J. Koo, O.D. Velev, Biomicrofluidics 7 (3) (2013) 031501.
[254] Y. Guo et al., Trends Chem. (2019).
[255] B.R. Moss, Ecology of Fresh Waters: Man and Medium, Past to Future, John Wiley & Sons, 2009.
[256] V.K. Gupta et al., RSC Adv. 2 (16) (2012) 6380.
[257] W. Cui et al., RSC Adv. 5 (65) (2015) 52966.
[258] X. Ji et al., J. Am. Chem. Soc. 140 (8) (2018) 2777.
[259] S. Lone et al., Environ. Sci. Water Res. Technol. 5 (1) (2019) 83.
[260] J. Ma et al., ACS Sustainable Chem. Eng. 5 (1) (2017) 843.
[261] D. Li et al., Chem. Commun. 47 (6) (2011) 1710.
[262] D. Li et al., Water Res. 47 (1) (2013) 209.
[263] W. Ali et al., Polymers 10 (2018) 6.
[264] X. Zhou et al., Energy Environ. Sci. 11 (8) (2018) 1985.
[265] F. Zhao et al., Nat. Nanotechnol. 13 (6) (2018) 489.
[266] P.A. Kallenberger, M. Fröba, Communications Chemistry 1 (1) (2018) 28.
[267] R. Li et al., Environ. Sci. Technol. 52 (19) (2018) 11367.
[268] K. Matsumoto et al., Nat. Commun. 9 (1) (2018) 2315.
[269] F. Zhao et al., Adv. Mater. 31 (10) (2019) 1806446.
[270] S. Ahuja, Handbook of Water Purity and Quality, Academic Press, 2009.
[271] G. Jing et al., Colloids Surf., A 416 (2013) 86.
[272] M. Barakat, Arab. J. Chem. 4 (4) (2011) 361.
[273] K. Yamashita et al., Polym. Adv. Technol. 14 (3–5) (2003) 189.
[274] Y. Zheng, A. Wang, J. Chem. Eng. Data 55 (9) (2010) 3494.
[275] J. Ma et al., Sci. Rep. 5 (2015) 13578.
[276] B. Vivek, E. Prasad, J. Phys. Chem. B 119 (14) (2015) 4881.
[277] V. Van Tran et al., Environ. Sci. Pollut. Res. 25 (25) (2018) 24569.
[278] P.M. Pakdel, S.J. Peighambardoust, J. Environ. Manage. 217 (2018) 123.
[279] P.M. Pakdel, S.J. Peighambardoust, Carbohydr. Polym. 201 (2018) 264.
[280] D. Li et al., Soft Matter 7 (21) (2011) 10048.
[281] A. Razmjou et al., Environ. Sci. Technol. 47 (12) (2013) 6297.
[282] X. Fan et al., Adv. Mater. 28 (21) (2016) 4156.
[283] D. Li, H. Wang, J. Mater. Chem. A 1 (45) (2013) 14049.
[284] Y. Cai, Desalination 391 (2016) 16.
[285] X. Zhou, et al., (2019) 5 (6), eaaw5484..
[286] Y. Guo et al., ACS Nano 13 (7) (2019) 7913.
[287] Y. Guo et al., Nano Lett. 19 (4) (2019) 2530.
[288] L.J. Mauer, L.S. Taylor, Annu. Rev. Food Sci. Technol. 1 (2010) 41.
[289] H. Kim et al., Science 356 (6336) (2017) 430.
[290] H. Kim et al., Nat. Commun. 9 (1) (2018) 1191.
[291] A. Rotzetter et al., Adv. Mater. 24 (39) (2012) 5352.
[292] R. Li et al., Environ. Sci. Technol. 52 (9) (2018) 5398.
[293] D. Seliktar, Science 336 (6085) (2012) 1124.
[294] F.N. Muya et al., Water Sci. Technol. 73 (5) (2016) 983.
[295] J. Knight et al., Opt. Lett. 21 (19) (1996) 1547.
[296] A.F. Prokop et al., Ultrasound Med. Biol. 29 (9) (2003) 1351.
[297] K. Zhang et al., Adv. Funct. Mater. (2019) 1903699.
[298] S. Xu et al., ACS Appl. Mater. Interfaces 10 (42) (2018) 36352.
[299] A. Shanker et al., Sci. Adv. 3 (7) (2017) e1700342.
[300] N. Tang et al., Polymers 9 (12) (2017) 688.
[301] S. Lin et al., Proc. Natl. Acad. Sci. U.S.A 116 (21) (2019) 10244.
[302] Y. Xu et al., Sci. Adv. 4 (3) (2018) eaar3031.
[303] X. Zhao, Y. Kim, Soft microbots programmed by nanomagnets, Nature Publishing Group, 2019.
[304] B.P. Lee et al., Annu. Rev. Mater. Res. 41 (2011) 99.
[305] A. Abramson et al., Science 363 (6427) (2019) 611.
[306] D. Michie et al., Neural Stat. Class. (1994) 13.
[307] X. Hou et al., Environ. Sci. Nano 5 (10) (2018) 2216.
[308] P. Raccuglia et al., Nature 533 (7601) (2016) 73.
[309] P. Casale et al., Human activity recognition from accelerometer data using a wearable device, in: Iberian Conference on Pattern Recognition and Image Analysis, Springer, 2011, p. 289.
[310] K.J. Kubota et al., Mov. Disord. 31 (9) (2016) 1314.
[311] N. Banka et al., Iterative machine learning for precision trajectory tracking with series elastic actuators, in: 2018 IEEE 15th International Workshop on Advanced Motion Control (AMC), IEEE, 2018, p. 234.
[312] J.P. Gong, Soft Matter 6 (12) (2010) 2583.
[313] R. Bai et al., Extreme Mech. Lett. 15 (2017) 91.
[314] J. Li et al., J. Mater. Chem. B 2 (39) (2014) 6708.
[315] X.P. Morelle et al., Adv. Mater. 30 (35) (2018) 1801541.
[316] R.H. Stokes, R.A. Robinson, J. Am. Chem. Soc. 70 (5) (1948) 1870.
[317] S.A. Asher, J.H. Holtz, Polymerized Crystalline Colloidal Array Sensor Methods, U.S. Patent and Trademark Office, Washington, DC, 1998.
[318] R.F. Stewart, Phase Change Sensor, U.S. Patent and Trademark Office, Washington, DC, 2010.
[319] R. Penterman et al., Temperature Sensor and Biosensor Using the Same, U.S. Patent and Trademark Office, Washington, DC, 2010.
[320] K.K. Parker, M. O'grady, Porous Electroactive Hydrogels and Uses Thereof, U.S. Patent and Trademark Office, Washington, DC, 2015.
[321] G. Rao et al., Ratiometric Fluorescent pH Sensor for Non-Invasive Monitoring, U.S. Patent and Trademark Office, Washington, DC, 2008.
[322] I.S. Han et al., Photometric Glucose Measurement System Using Glucose-Sensitive Hydrogel, U.S. Patent and Trademark Office, Washington, DC, 2004.
[323] J.Y. Sun et al., Stretchable Ionics for Transparent Sensors and Actuators, U.S. Patent and Trademark Office, Washington, DC, 2016.
[324] J.A. Lewis, A.S. Gladman, Method of 4d Printing A Hydrogel Composite Structure, U.S. Patent and Trademark Office, Washington, DC, 2017.
[325] J. Aizenberg et al., Environmentally Responsive Optical Microstructured Hybrid Actuator Assemblies and Applications Thereof, U.S. Patent and Trademark Office, Washington, DC, 2016.
[326] J. Kim et al., Dual Stimuli-Responsive Hydrogels and Their Synthetic Methods, U.S. Patent and Trademark Office, Washington, DC, 2004.
[327] H. Jiang et al., Infrared Light-and Thermal-Responsive Graphene Oxide Hydrogel Polymer Composites, U.S. Patent and Trademark Office, Washington, DC, 2015.
[328] S. Daunert et al., Artificial Muscle Hydrogel Blends Reversibly Electroactuated Near Neutral pH, Implantable Actuating Devices, and Methods Using the Same, U.S. Patent and Trademark Office, Washington, DC, 2009.
[329] D.J. Mooney, X. Zhao, Active Scaffolds for On-Demand Drug and Cell Delivery, U.S. Patent and Trademark Office, Washington, DC, 2015.
[330] S. Richardson-Burns et al., Co-electrodeposited hydrogel-conducting polymer electrodes for biomedical applications, U.S. Patent and Trademark Office, Washington, DC, 2015.
[331] M. Palasis, Multi-balloon Catheter with Hydrogel Coating, U.S. Patent and Trademark Office, Washington, DC, 2006.
[332] R. Janssen et al., Gloves with Hydrogel Coating for Damp Hand Donning and Method of Making Same, U.S. Patent and Trademark Office, Washington, DC, 2006.
[333] A. Rosenthal et al., Triggered Release Hydrogel Drug Delivery System, U.S. Patent and Trademark Office, Washington, DC, 2006.
[334] A. Childs et al., Sci. Rep. 6 (2016) 34905.
[335] J. Iwata et al., Silicone hydrogel contact lens, U.S. Patent and Trademark Office, Washington, DC, 2006.
[336] P.L. Valint Jr et al., Surface Treatment of Silicone Hydrogel Contact Lenses Comprising Hydrophilic Polymer Chains Attached to an Intermediate Carbon Coating, U.S. Patent and Trademark Office, Washington, DC, 2003.
[337] L. Edwards et al., Tactile-Feedback Touch Screen, U.S. Patent and Trademark Office, Washington, DC, 2013.
[338] M.-G. Shim et al., Smart Window, U.S. Patent and Trademark Office, Washington, DC, 2013.
[339] K.A. Deisseroth et al., RNA Fixation and Detection in CLARITY-based Hydrogel Tissue, U.S. Patent and Trademark Office, Washington, DC, 2019.
[340] Y. Ahn et al., ACS Appl. Mater. Interfaces 6 (21) (2014) 18401.
[341] N. Annabi et al., Adv. Mater. 28 (1) (2016) 40.
[342] X. Xiao et al., Polymers 9 (7) (2017) 259.
[343] P. Keusch, J.L. Essmyer, Conductive Adhesive Medical Electrode Assemblies, U. S. Patent and Trademark Office, Washington, DC, 1988.
[344] S. Sekine et al., J. Am. Chem. Soc. 132 (38) (2010) 13174.
[345] M.R. Abidian, D.C. Martin, Adv. Funct. Mater. 19 (4) (2009) 573.
[346] Y. Xu et al., ACS Appl. Mater. Interfaces 10 (17) (2018) 14418.
[347] S. Naficy et al., Chem. Mater. 24 (17) (2012) 3425.
[348] O. Ozay et al., Desalination 260 (1–3) (2010) 57.

[349] C.F. Degiorgi et al., Radiat. Phys. Chem. 63 (1) (2002) 109.
[350] A.M. Atta et al., J. Appl. Polym. Sci. 123 (4) (2012) 2500.
[351] H.G. Park et al., Alginate Gel Based Adsorbents for Heavy Metal Removal, U.S. Patent and Trademark Office, Washington, DC, 2006.
[352] X. Zhou et al., Sci. Adv. 5 (6) (2019) eaaw5484.
[353] Y. Cai et al., Water Res. 47 (11) (2013) 3773.
[354] A. Razmjou et al., Chem. Eng. J. 215 (2013) 913.
[355] X. Hu et al., A Draw Solute and an Improved Forward Osmosis Method, U.S. Patent and Trademark Office, Washington, DC, 2016.
[356] Z. L. Wu et al., Adv. Healthcare Mater. (2020) 1901396. https://doi.org/10.1002/adhm.201901396.
[357] S. Fuchs et al., Adv. Healthcare Mater. (2020) 1901396. https://doi.org/10.1002/adhm.201901396.